MYCOLOGIA

Vol. 105 No. 6

November December 2013

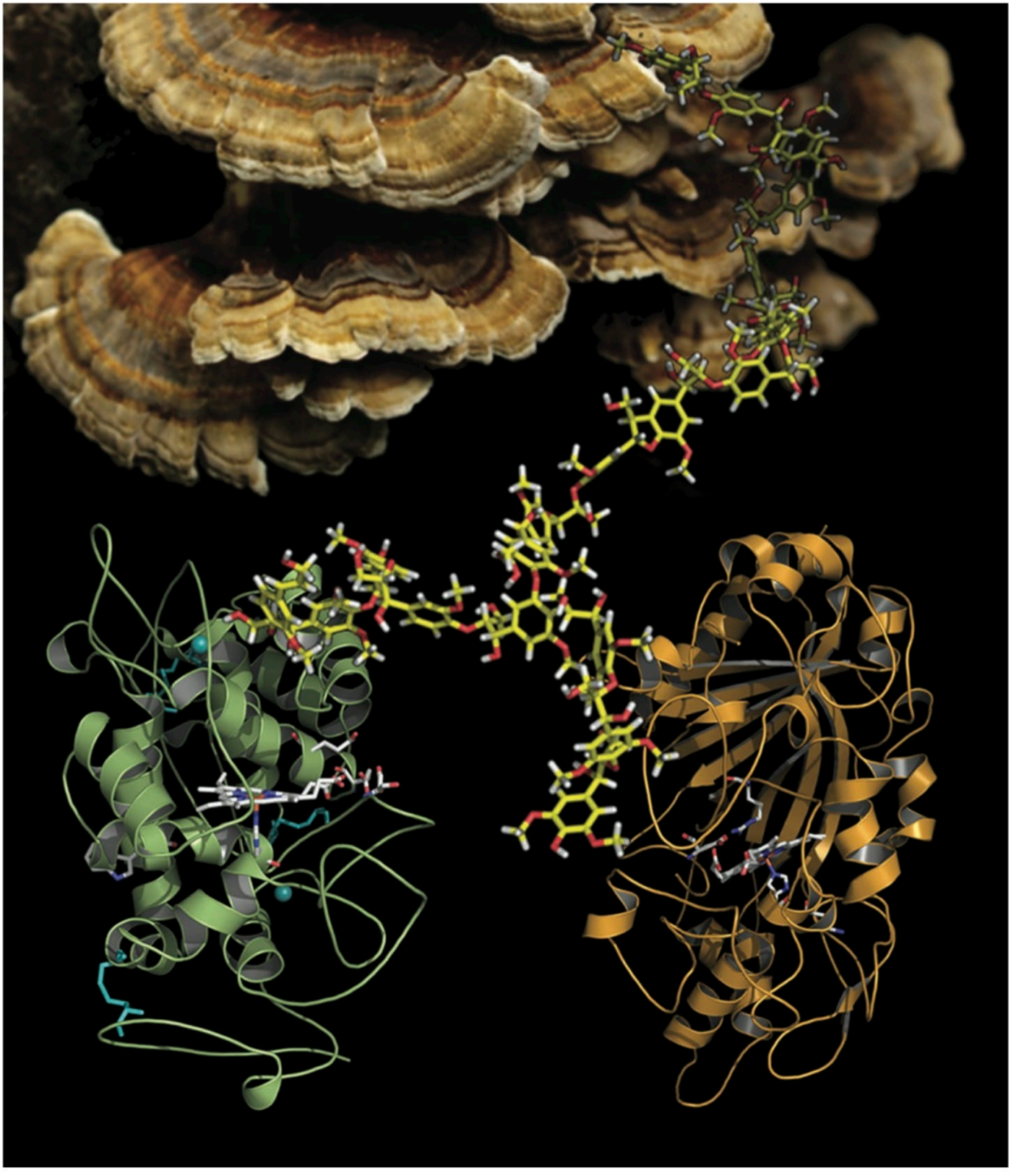

OFFICIAL BIMONTHLY PUBLICATION *of the* MYCOLOGICAL SOCIETY OF AMERICA

Mycologia, 105(6), 2013, pp. 1350–1373. DOI: 10.3852/13-003

Phylogenetic and phylogenomic overview of the Polyporales

Manfred Binder[1]
Biology Department, Clark University, 950 Main Street, Worcester, Massachusetts 01610, and CBS-KNAW Fungal Biodiversity Centre, Uppsalalaan 8, 3584 CT, Utrecht, the Netherlands

Alfredo Justo[1]
Biology Department, Clark University, 950 Main Street, Worcester, Massachusetts 01610

Robert Riley
Asaf Salamov
US Department of Energy Joint Genome Institute, 2800 Michell Drive, Walnut Creek, California 94598

Francesc Lopez-Giraldez
Department of Ecology and Evolutionary Biology, Yale University, Osborne Memorial Labs 226, 165 Prospect Street, New Haven, Connecticut 06520-8106

Elisabet Sjökvist
Deptartment of Biological and Environmental sciences, University of Gothenburg, PO Box 461, SE 40530 Göteborg, Sweden

Alex Copeland
Brian Foster
Hui Sun
US Department of Energy Joint Genome Institute, 2800 Michell Drive, Walnut Creek, California 94598

Ellen Larsson
Deptment of Biological and Environmental sciences, University of Gothenburg, PO Box 461, SE 40530 Göteborg, Sweden

Karl-Henrik Larsson
Natural History Museum, University of Oslo, PO Box 1172 Blindern, NO 0318 Oslo, Norway

Jeffrey Townsend
Department of Ecology and Evolutionary Biology, Yale University, Osborne Memorial Labs 226, 165 Prospect Street, New Haven, Connecticut 06520-8106

Igor V. Grigoriev[2]
US Department of Energy Joint Genome Institute, 2800 Michell Drive, Walnut Creek, California 94598

David S. Hibbett[2]
Biology Department, Clark University, 950 Main Street, Worcester, Massachusetts 01610

Abstract: We present a phylogenetic and phylogenomic overview of the Polyporales. The newly sequenced genomes of *Bjerkandera adusta*, *Ganoderma* sp., and *Phlebia brevispora* are introduced and an overview of 10 currently available Polyporales genomes is provided. The new genomes are 39 500 000–49 900 00 bp and encode for 12 910–16 170 genes. We searched available genomes for single-copy genes and performed phylogenetic informativeness analyses to evaluate their potential for phylogenetic systematics of the Polyporales. Phylogenomic datasets (25, 71, 356 genes) were assembled for the 10 Polyporales species with genome data and compared with the most comprehensive dataset of Polyporales to date (six-gene dataset for 373 taxa, including taxa with missing data). Maximum likelihood and Bayesian phylogenetic analyses of genomic datasets yielded identical topologies, and the corresponding clades also were recovered in the 373-taxa dataset although with different support values in some datasets. Three previously recognized lineages of Polyporales, antrodia, core polyporoid and phlebioid clades, are supported in most datasets, while the status of the residual polyporoid clade remains uncertain and certain taxa (e.g. *Gelatoporia*, *Grifola*, *Tyromyces*) apparently do not belong to any of the major lineages of Polyporales. The most promising candidate single-copy genes are presented, and nodes in the Polyporales phylogeny critical for the suprageneric taxonomy of the order are identified and discussed.

Key words: genomics, new molecular markers, Polyporales, taxonomy

Introduction

The Polyporales is a diverse group of Agaricomycetes including roughly 1800 described species (Kirk et al. 2008). They are key players in the carbon cycle, and the white-rot members of the order are among the most efficient lignin decayers in the biosphere (Floudas et al. 2012). Advances in our understanding of the biodiversity and ecology of this group can be achieved only if coupled with a comprehensive phylogeny for the Polyporales, which brings us back to a long-standing question in systematics: more genes or more taxa? Here we explore both solutions to the problem, which involves the use of whole genome sequence data in comparison to extensively sampled multigene datasets.

A wide variety of basidiocarp types and hymenophore configuration in the Polyporales include bracket-shaped (e.g. *Ganoderma, Trametes*), effused

Submitted 3 Jan 2013; accepted for publication 29 Apr 2013.

[1] Authors contributed equally to this work.

[2] Corresponding author. E-mail: ivgrigoriev@lbl.gov; dhibbett@clarku.edu

resupinate (*Wolfiporia*, *Phlebia*), stipitate with poroid (*Polyporus*) lamellate (*Lentinus*) or smooth (*Podoscypha*) hymenophores. A few species produce shelf-like or flabellate clusters of overlapping basidiocarps (*Laetiporus*, *Sparassis*). Variations of and transitions between basidiocarp types exist, and there is no morphological synapomorphy that unites the Polyporales (Binder et al. 2005). The most common ''polyporoid'' basidiocarps types just mentioned also have evolved convergently in at least 11 additional orders of Agaricomycetes (e.g. *Gloeophyllum* [Gloeophyllales], *Phellinus* [Hymenochaetales], *Heterobasidion* [Russulales] etc.) (Hibbett 2007).

The great majority of Polyporales are saprotrophic wood-decay fungi, while a few are plant pathogens causing timber damage (e.g. *Fomitopsis*, *Ganoderma*, *Phaeolus*). Wood-decayers in the Polyporales can be divided into two major groups: white-rot fungi that are able to decay both lignin and cellulosic compounds and brown-rot fungi that have taken a less costly approach to access cellulose and hemicellulose by either impairing the structural integrity of lignin using oxidative enzymes or secondary metabolites to produce hydrogen peroxide and free radicals (Eastwood et al. 2011). White-rot species allow the carbon in lignin to become readily available in the form of CO_2, which in turn feeds into biogeochemical reactions or functions as substrate for other organisms. Brown-rot species on the other hand leave behind residual lignin that is mostly inert to further microbial and fungal decay for extended periods and leads to carbon sequestration. The enzymatic capabilities of the Polyporales are not only important for the biogeochemical cycles but also make them prime candidates for industrial applications including biomass conversion, mycoremediation, paper pulping and the production of biofuels.

Resolving the taxonomic structure of Polyporales has proven difficult based on the nearly exclusive use of ribosomal DNA sequences (e.g. Binder et al. 2005). More recent studies (e.g. Justo and Hibbett 2011, Miettinen et al. 2011, Sjökvist et al. 2012) have used also protein-coding genes (*rpb1, rpb2, tef1*) for phylogenetic reconstruction showing that many genera and families belonging to the Polyporales are poly- and/or paraphyletic as currently defined. To achieve a taxonomic arrangement of the Polyporales that truly reflects the evolutionary history of the group a collective effort and coordination among researchers will be necessary, especially concerning two different aspects: (i) the building of a well resolved phylogeny ideally should be based on an identical set of genes for as many taxa as possible, with attention to nodes and clades that have been difficult to resolve in the past, and taxa of nomenclatural relevance (type genera and species); (ii) the ''translation'' of the phylogeny into a formal subordinal taxonomy also will require a general consensus about how broadly or narrowly families and genera should be defined. This effort should start with the reevaluation and possibly validation of clade names that have been introduced informally to facilitate communication, such as core polyporoid clade, antrodia clade, phlebioid clade, residual polyporoid clade and cinereomyces clade (Hibbett and Donoghue 1995, Larsson et al. 2004, Binder et al. 2005, Garcia-Sandoval et al. 2010, Miettinen et al. 2011). Justo and Hibbett (2011) further subdivided the core polyporoid clade into three well supported lineages (polyporus, trametoid, dentocorticium clades) without any judgment on the suprageneric taxonomy of this group. Studies using the combined 5.8S and ribosomal nuclear ribosomal LSU DNA (Larsson 2007) or multigene datasets (Miettinen et al. 2011) explored the application of already existing family names. There are 40 validly published and legitimate family names for taxa belonging (or putatively belonging) in the Polyporales (TABLE I). The oldest name is *Polyporaceae* (1839) and the most recent is *Phaeotrametaceae* (2005), but the great majority of family names, a total of 29, were published by Jülich (1981) although, with the exception of *Fomitopsidaceae* and *Phaneorochaetaceae*, they rarely have been used since their creation.

Under the auspices of the Joint Genome Institute (JGI) Fungal Genomics Program (Grigoriev et al. 2011), fungal phylogenomics has experienced rapid advances in recent years. The first sequenced Basidiomycota genome was a member of the Polyporales, the white-rot *Phanerochaete chrysosporium* (Martinez et al. 2004). The data from the genome of *P. chrysosporium* influenced the research of biologists, biochemists and computer scientists alike and allowed the first insight into the white-rot mechanism. This opened the door for comparative genomics with the non-ligninolytic, brown rot-producing *Rhodonia placenta* (= *Postia placenta*) (Martinez et al. 2009) and the white-rot *Gelatoporia subvermispora* (= *Ceriporiopsis subversmispora*) (Fernandez-Fueyo et al. 2012), which in contrast to *P. chrysosporium* delignifies wood selectively. Four other Polyporales genomes (*Dichomitus squalens*, *Fomitopsis pinicola*, *Trametes versicolor*, *Wolfiporia cocos*) were generated in the Saprotrophic Agaricomycotina Project (SAP), which focused on the evolution of the wood-decay apparatus (Floudas et al. 2012), and other independent projects also are contributing new genomes (e.g. Chen et al. 2012) with *Ganoderma lucidum*.

In the present paper we bring together phylogenomics and phylogenetics to provide an overview of

TABLE I. Legitimate family names for taxa belonging (or putatively belonging) in the Polyporales

Family	Type species of the type genus	Phylogenetic position
1. *Dacryobolaceae* Jülich 1981	*Dacryobolus sudans* (Alb. & Schwein.) Fr.	Antrodia clade
2. *Daedaleaceae* Jülich 1981	*Daedalea quercina* (L.) Pers.	Antrodia clade
3. *Fomitopsidaceae* Jülich 1981	*Fomitopsis pinicola* (Sw.) P. Karst.	Antrodia clade
4. *Laricifomitaceae* Jülich 1981	*Laricifomes officinalis* (Batsch) Kotl. & Pouzar	Antrodia clade
5. *Phaeolaceae* Jülich 1981	*Phaeolus schweinizii* (Fr.) Pat.	Antrodia clade
6. *Piptoporaceae* Jülich 1981	*Piptoporus betulinus* (Bull.) P. Karst.	Antrodia clade
7. *Sparassidaceae* Herter 1910	*Sparassis crispa* (Wulfen) Fr.	Antrodia clade
8. *Coriolaceae* Singer 1961	*Coriolus versicolor* (L.) Quél.	Core polyporoid clade
9. *Cryptoporaceae* Jülich 1981	*Cryptoporus volvatus* (Peck) Shear	Core polyporoid clade
10. *Echinochaetaceae* Jülich 1981	*Echinochaete brachypora* (Montagne) Ryvarden	Core polyporoid clade
11. *Fomitaceae* Jülich 1981	*Fomes fomentarius* (L.) Fr.	Core polyporoid clade
12. *Ganodermataceae* (Donk) Donk 1948	*Ganoderma lucidum* (Curtis) P. Karst.	Core polyporoid clade
13. *Grammotheleaceae* Jülich 1981	*Grammothele lineata* Berk. & M.A. Curtis	Core polyporoid clade
14. *Microporaceae* Jülich 1981	*Microporus xanthopus* (Fr.) Kuntze	Core polyporoid clade
15. *Pachykytosporaceae* Jülich 1981	*Pachykytospora tuberculosa* (Fr.) Kotl. & Pouzar	Core polyporoid clade
16. *Perenniporiaceae* Jülich 1981	*Perenniporia medulla-panis* (Jacq.) Donk	Core polyporoid clade
17. *Polyporaceae* Corda 1839	*Polyporus tuberaster* (Jacq. ex Pers.) Fr. [a]	Core polyporoid clade
18. *Sparsitubaceae* Jülich 1981	*Sparsitubus nelumbiformis* L.W. Hsu & J.D. Zhao	Core polyporoid clade
19. *Trametaceae* Boidin, Mugnier & Canales 1998	*Trametes suaveolens* (L.) Fr.	Core polyporoid clade
20. *Bjerkanderaceae* Jülich 1981	*Bjerkandera adusta* (Willd.) P. Karst.	Phlebioid clade
21. *Climacodontaceae* Jülich 1981	*Climacodon septentrionalis* (Fries) P. Karsten	Phlebioid clade
22. *Hapalopilaceae* Jülich 1981	*Hapalopilus rutilans* (Pers.) Murrill	Phlebioid clade
23. *Irpicaceae* Spirin & Zmitr. 2003	*Irpex lacteus* (Fr.) Fr.	Phlebioid clade
24. *Meruliaceae* Rea 1922	*Merulius tremellosus* Schrad	Phlebioid clade
25. *Phanerochaetaceae* Jülich 1981	*Phanerochaete velutina* (DC.) P. Karst.	Phlebioid clade
26. *Phlebiaceae* Jülich 1981	*Phlebia radiata* Fr.	Phlebioid clade
27. *Hyphodermataceae* Jülich 1981	*Hyphoderma setigerum* (Fr.) Donk	Residual polyporoid clade
28. *Meripilaceae* Jülich 1981	*Meripilus giganteus* (Pers.) P. Karst	Residual polyporoid clade
29. *Podoscyphaceae* D.A. Reid 1965	*Podoscypha nitidula* (Berk.) Pat.	Residual polyporoid clade
30. *Steccherinaceae* Parmasto 1968	*Steccherinum ochraceum* (Pers. ex J.F. Gmel.) Gray	Residual polyporoid clade
31. *Mycorrhaphiaceae* Jülich 1981	*Mycorrhaphium adustum* (Schwein.) Maas Geest.	Residual polyporoid clade (according to Miettinen et al. 2011)
32. *Grifolaceae* Jülich 1981	*Grifola frondosa* (Dicks.) Gray	Uncertain based on molecular data (probably in or close to the core polyporoid clade)
33. *Ischnodermataceae* Jülich 1981	*Ischnoderma resinosum* (Schrad.) P. Karst	Uncertain based on molecular data (probably in or close to the residual polyporoid clade)
34. *Rigidoporaceae* Jülich 1981	*Rigidoporus lineataus* (Pers.) Ryvarden	No data available for the type species (probably in or close to the residual polyporoid clade)
35. *Lophariaceae* Boidin, Mugnier & Canales 1998	*Lopharia mirabilis* (Berk. & Broome) Pat.	Uncertain
36. *Diachanthodaceae* Jülich 1981	*Diacanthodes novo-guineensis* (Hennings) O. Fidalgo	Unknown
37. *Incrustoporiaceae* Jülich 1981	*Incrustoporia stellae* (Pilát) Domanski	Unknown
38. *Nigrofomitaceae* Jülich 1981	*Nigrofomes melanoporus* (Mont.) Murrill	Unknown
39. *Phaeotrametaceae* Popoff ex Piatek 2005	*Phaeotrametes decipiens* (Berk.) J.E. Wright	Unknown
40. *Haddowiaceae* Jülich 1981	*Haddowia longipes* (Lév.) Steyaert	Unknown (probably = *Ganodermataceae*)

[a] *Polyporus tuberaster* is accepted here as the type species of *Polyporus*, but see also Krüger and Gargas (2004) and Sotome et al. (2008) for a detailed discussion on the problems surrounding the typification of *Polyporus*.

evolutionary relationships in the Polyporales that will serve as road map for future studies in both fields. Our particular foci are: (i) We introduce de novo sequenced genomes of the three white-rot Polyporales species, *Bjerkandera adusta*, *Ganoderma* sp. (*lucidum* complex) and *Phlebia brevispora*; (ii) we use the 10 Polyporales genomes currently available for identification and informativeness profiling of single-copy genes as candidates for future phylogenetic studies in the Polyporales; (iii) we assemble core (nearly complete) and extended (taxa introducing missing data) super matrices with the six AFTOL1 (http://aftol.org/) target regions (5.8S, nrLSU, nrSSU, *rpb1*, *rpb2*, *tef1*), combining published data and newly generated sequences to the largest dataset available of Polyporales to date. We also compare the results from these datasets with three different phylogenomic datasets of the Polyporales (25, 71, 356 genes respectively). Analyses of lignin-degrading peroxidases in Polyporales and other functional aspects are described in accompanying papers (e.g. Ruiz-Dueñas et al. this issue) as well as taxonomic studies on the antrodia clade (Ortiz-Santana et al. this issue).

MATERIALS AND METHODS

New genomes: sources of strains, culture conditions and extraction of nucleic acids.—Cultures of *Bjerkandera adusta* (strain HHB-12826-SP), *Ganoderma* sp. (strain 10597 SS1) and *Phlebia brevispora* (strain HHB-7030) were cultivated in the Hibbett laboratory at Clark University. All cultures are available from the Northern Research Station Laboratory (formerly Forest Products Laboratory, USDA Forest Service, Madison, Wisconsin). These cultures were grown routinely under ambient laboratory conditions at 23 C in daylight and simultaneously in an incubator (Precision, GCA, Thermo Scientific, Asheville, North Carolina) at 28 C in the dark. Liquid nutrient media were used to determine the optimal growth conditions for the fungal isolates, including modified vitamin (VIT) medium (1), potato-dextrose (PD) medium (24 g potato-dextrose [EMD]/L), malt extract (ME) medium (20 g malt extract, 0.5 g yeast extract/L), minimal (MM) medium (0.25 g ammonium tartrate, 0.5 g glucose, 0.5 g yeast extract/L) and Avicel medium (40 g Avicel PH-101 from Fluka analytical, 5 g ammonium tartrate,1 g KH_2PO_4, 0.5 g $MgSO_4$ [$\times$ $7H_2O$], 0.001 g $CaCl_2$ [$\times$ $2H_2O$], 0.1 g yeast extract, 0.88 mg $ZnSO_4$ [$\times$ $7H_2O$], 0.81 mg $MnSO_4$ [$\times$ $4H_2O$], 0.80 mg $FeCl_3$ [$\times$ $6H_2O$]/L). Mycelium used for DNA extractions was grown 1–2 wk and was harvested with a system including a Buchner funnel and Whatman No. 4 filter disks. Up to 10 g (wet) ground mycelium powder were loaded on QIAGEN (Valencia, California) Genomic 500/G tips and processed according to the lysis protocol for tissue in the QIAGEN Blood & Cell Culture DNA Kit, including the RNase and Proteinase K steps. Materials for RNA extraction were filtered after 3–5 d growth. The QIAGEN RNeasy Midi Kit was used to process up to 1 g (wet) of ground mycelium at a time. The extraction followed the protocol for isolation of total RNA from animal tissues (QIAGEN) including on-column DNase digestion and final standard LiCl purification.

Genome sequencing, assembly and automated annotation.—Genomes were sequenced with a hybrid whole-genome shotgun approach using a combination of ABI3730 (fosmids) (Applied Biosystems, Foster City, California), 454-Titanium (454 Life Sciences, Branford, Connecticut) and Illumina GAII (Illumina Inc., San Diego, California) sequencing platforms. Roche 454 sequence was from one or more standard libraries and typically one 4 kb and one 8 kb paired-end library. Illumina reads were collected from nominal 300 bp fragment libraries, sequenced to 76 bp and assembled with Velvet (0.7.55 - REF). The resulting Velvet contigs were shredded into overlapping 800 bp chunks with a 200 bp overlap and used by Newbler (2.5-internal-10Apr08-1) together with 454 standard and paired-end reads and Sanger-sequenced fosmids ends. Gaps were closed in silico with gap resolution. cDNA libraries were constructed with the methods outlined in the Roche cDNA Rapid Library Preparation Method Manual (Roche). The 454 libraries were sequenced with the genome sequencer FLX Instrument (Roche). Ribosomal RNA, low quality and low complexity reads were filtered out, then the remaining reads were assembled with either a JGI specific assembly process or Newbler (2.3-PreRelease-6/30/2009, Roche) with default parameters. Each of the JGI-sequenced genomes introduced here were annotated with the JGI annotation pipeline, which takes multiple inputs (scaffolds, ESTs, known genes) and runs several analytical tools for gene prediction and annotation, and deposits the results in Mycocosm (http://jgi.doe.gov/fungi) for further analysis and manual curation. All genome assemblies and annotations can be accessed interactively through the JGI fungal genome portal Mycocosm (Grigoriev et al. 2012) at http://jgi.doe.gov/fungi. The three new Polyporales genomes discussed here also are deposited to DDBJ/EMBL/GenBank under these accessions numbers: *Phlebia brevispora* HHB-7030 SS6: ANLB00000000, *Ganoderma* sp. 10597 SS1: ANLC00000000, and *Bjerkandera adusta* HHB-12826-SP SB-22: ANLD00000000.

Identification of single-copy genes.—A cluster was assembled in the JGI Mycocosm for the 10 Polyporales genomes available as of Jun 2012 (No. 1262): *Bjerkandera adusta*, *Dichomitus squalens*, *Fomitopsis pinicola*, *Ganoderma* sp. (*G. lucidum* complex), *Gelatoporia subvermispora* (= *Ceriporiopsis subvermispora*), *Phanerochaete chrysosporium*, *Phlebia brevispora*, *Rhodonia placenta* (= *Postia placenta*), *Trametes versicolor* and *Wolfiporia cocos*. BLAST queries in InParanoid (http://inparanoid.sbc.su.se/cgi-bin/index.cgi) and the *Saccharomyces* Genome Database (http://www.yeastgenome.org/) were used to identify the putative orthologs in yeast. KEGG (http://www.genome.jp/kegg/) was used to estimate the higher level functions of the single-copy genes. An ad hoc cluster (No. 1263) was assembled to check for the presence of the identified single-copy genes in the selected outgroups for the phylogenomic analyses: *Fomitiporia*

mediterranea (Hymenochaetales), *Gloeophyllum trabeum* (Gloeophyllales), *Heterobasidion annosum* (Russulales), *Punctularia strigosozonata* (Corticiales), *Stereum hirsutum* (Russulales).

Phylogenomic analyses.—Two datasets were assembled: (i) A 356-gene dataset that combines single-copy genes present in the 10 Polyporales + 5 outgroup dataset obtained from genome data; (ii) Combined 71-gene based on the AFTOL2 genes dataset (Floudas et al. 2012). In both cases amino acid sequences were aligned with MAFFT 6 (Katoh et al. 2005) under the L-INS-I setting and curated with Gblocks under stringent settings (Castresana 2000, Talavera and Castresana 2007). The 356-gene dataset was analyzed under the maximum likelihood criterion (ML) with RAxML 7.2.6 (Stamatakis 2006) and the 71-gene dataset with both ML and Bayesian (BY) PhyloBayes 3 (Lartillot et al. 2009) analyses. We also constructed a third dataset with the 25 genes that performed best in the informativeness profiling analysis (see below), which was analyzed with both ML and Bayesian methods. Searches conducted with RAxML involved 100 rapid bootstrap replicates and ML optimization using the PROTGAMMAWAGF model. This model specifies the WAG amino acid matrix with the Γ model of rate heterogeneity using four discrete rate categories, while RAxML estimates all free model parameters. PhyloBayes was run with the CAT infinite mixture model accounting for site-specific amino acid preferences, employing six MCMC chains sampling data every 1000th cycle. The Bayesian analyses were set to stop after the maximum differences in split frequency between runs reached zero and consensus trees were built with the READPB command.

Informativeness profiling.—To evaluate the potential use of the identified single-copy genes for phylogenetic reconstruction we profiled their phylogenetic informativeness. To compute the rates of evolution of amino acid and nucleotide sites, we specified an ultrametric evolutionary tree. The concatenated amino acid sequences (257 297 aa) were used to estimate the phylogeny with the parallel version of PhyML 20110919 (Guindon and Bascon 2003, Guindon 2010). The LG model was selected assuming an estimated proportion of invariant sites and four gamma-distributed rate categories to account for rate heterogeneity across sites. Equilibrium amino acid frequencies were estimated from the model. We let PhyML optimize substitution model parameters. We used a time-calibrated phylogeny (ultrametric tree). While absolute dates of internal nodes were not relevant to any inferences herein, their relative depths were aligned with the ultrametric profiles for predictive purposes. We obtained the chronogram by passing the phylogenetic tree to r8s software 1.71 (Sanderson 2003). We pruned *Fomitiporia mediterranea* (further root), and the place where this outgroup attached to the rest of the tree became the root node for r8s. We fixed the age of the root to 1. Node heights were estimated by nonparametric rate smoothing (NPRS) with a truncated Powell algorithm in r8s.

Using the alignment data and the ultrametric tree, molecular evolutionary rates were estimated for each gene at each alignment position independently. We used Rate4-site (Mayrose et al. 2005) and HyPhy (Pond et al. 2005) to obtain the substitution rates at amino acid and nucleotide sites respectively. In the Rate4site program rates were inferred by ML assuming a JTT model for the topology and branch lengths of the input phylogenetic tree without any optimization. In the HyPhy analysis we assumed a Kimura-2-parameter (K2P) model with transitions twice as likely as transversions.

For each gene, the phylogenetic informativeness profile ρ as a function of time, T, was calculated, substituting the estimated rates λi of evolution of each site (Townsend 2007). This formula provides a metric of the probability that character i would provide an unambiguous synapomorphy lying within an asymptotically short internode between two pairs of sister taxa whose common ancestor is at time T. To convey the informativeness of a particular dataset, the equation was plotted at a continuum of depths, from time 0 to the root, of the phylogenetic trees. The differential phylogenetic informativeness (DPI) of each gene was evaluated quantitatively by integrating on the phylogenetic informativeness profile from the origin (h1) to the terminus (h) of the epochs of interest. Three epochs of interest were used: 0.17–0.49 (from the appearance of the antrodia clade to the most recent split on the tree between *Ganoderma* sp. and *Dichomitus squalens*), 0.49–0.77 (from the origin of the Polyporales to the origin of the antrodia clade) and 0.77–1 (previous to the appearance of the Polyporales). Using DPI, we ranked the genes for each one of the epochs. Both the calculations of the molecular evolutionary rate and the phylogenetic informativeness profiles were performed with the PhyDesign web application (López-Giráldez and Townsend 2011).

To quantify phylogenetic noise as well as signal and calculate a probability of resolution for each gene for the indicated node (t = 0.06, T = 0.68), we applied the analytical solution for probability of resolution from Townsend et al. (2012). Once probabilities of resolution were calculated for the three nodes indicated above we calculated: (i) best overall gene: as the most likely to provide accurate resolution over all three epochs (product of the probabilities); (ii) worst overall gene: as the one most likely to get all three epochs incorrect. (product of [1-the probabilities]); (iii) best recent yet worst ancient was calculated as the ratio of rankings in ancient Pr (probability of resolution) over recent Pr; (iv) best ancient yet worst recent was calculated as the ratio of rankings in recent Pr over ancient Pr.

Rates of DNA and amino acid site evolution were estimated as above. For nucleotide characters, we calculated the results using their nominal state space (four states). For amino acid characters, we used an empirical estimate of their state space (five states; Simmons et al. 2004).

Multigene phylogenetic overview of the Polyporales.—Two major datasets, an extended supermatrix and a core supermatrix, were analyzed. The extended supermatrix combines almost all nrLSU, 5.8S, nrSSU, *rpb1*, *rpb2* and *tef1* data for the Polyporales publicly available in GenBank by the end of Dec 2011 (excluding different copies of the same locus for different isolates of the same species). Only

TABLE II. Assembly statistics for the three new Polyporales genomes

	Bjerkandera adusta	*Ganoderma* sp.	*Phlebia brevispora*
Genome assembly length, Mbp	42.73	39.52	49.96
Number of scaffolds	508	156	1645
Scaffold N50/L50(Mbp)	13/1.03	6/2.73	329
Total contig length, Mbp (percent gap)	40.23(5.8%)	38.53(2.5%)	46.43(7%)
Number of contigs	1263	503	3178
Contig N50/L50(Kbp)	88/124.7	27/375.6	104/66.2
Percent repeats	1.34%	2.53%	4.53%

one set of sequences for any given taxon was included (SUPPLEMENTARY TABLE I). Whenever possible the loci were selected from the same isolate; if not possible the conspecificity of different isolates was assessed indirectly by comparison of loci in common for both isolates and/or the results of BLAST queries. Additional newly generated nrLSU, *rpb2* and *tef1* for selected taxa of Polyporales also were included (SUPPLEMENTARY TABLE II). These sequences were generated with standard DNA extraction, PCR and sequencing methods (e.g. Sjökvist et al. 2012). For the 10 Polyporales and two outgroup species with genomes available the complete sequences for *rpb1, rpb2* and *tef1* extracted from the genome data were used. The supermatrix consists of 373 Polyporales taxa, which are represented by at least nrLSU data, except seven species with *rpb2* but no nrLSU data. Two hundred sixty 5.8S, 91 nrSSU, 44 *rpb1*, 130 *rpb2* and 86 *tef1* were concatenated to the nrLSU data. *Stereum hirsutum* and *Heterobasidion annosum* (Russulales) were used as outgroup taxa. To test for possible conflicts ML analyses were performed in a dataset with ribosomal genes only (nrLSU, 5.8S, nrSSU) and compared to a separate datasets for each protein-coding gene (both nucleotide and amino acid datasets).

The core supermatrix excludes from the extended supermatrix all taxa that lack data for both *rpb1* and *rpb2*. It has 126 Polyporales taxa. For both datasets, maximum likelihood and Bayesian analyses were run. Maximum likelihood analyses (ML) were run in the RAxML servers, 7.2.8 (Stamatakis et al. 2008), under a GTR model with 100 rapid bootstrap replicates. Bayesian analyses (BY) were run with MrBayes 3.2 (Ronquist et al. 2012) for 10 000 000 generations, with four chains, and trees sampled every 100 generations. The initial burn-in was set to 2 500 000 generations, and after examining the graphic representation of the likelihood scores of the sampled trees that was confirmed to be an adequate value for both datasets. A 50% majority rule consensus tree was computed with the remaining trees.

RESULTS

Polyporales genomes.—A general characterization of the genomes of *Bjerkandera adusta*, *Ganoderma* sp. and *Phlebia brevispora* is provided (TABLES II, assembly statistics; III, gene model statistics; IV, EST and protein similarity support; V, KOG and KEGG characterization).

Genome sizes and gene counts of sequenced Polyporales are 35 000 000–50 000 000 bp and 10 000–16 000 genes respectively. The first species of Polyporales to have its genome sequenced, *Phanerochaete chrysosporium* (Martinez et al. 2004), is also the smallest with 35 100 000 bp and 10 048 genes. These numbers correlate in general (SUPPLEMENTARY FIG. 1), but repeats, primarily transposable elements, can introduce significant variation into the genome size. The 50 500 000-bp genome of *Wolfiporia cocos* is the largest among the Polyporales and contains more than 10% repetitive elements and only 12 746 genes. In contrast, the next largest genome of *Phlebia brevispora* (49 960 000 bp) encodes for the largest number of genes (16 170) among the Polyporales.

The 10 sequenced Polyporales offer a range of evolutionary distances reflected in gene content and similarities between pairwise orthologs. The closest pair of Polyporales, *Ganoderma* sp. and *Dichomitus squalens*, share 8137 orthologs with average amino

TABLE III. Predicted gene model statistics for the three new Polyporales

	Bjerkandera adusta	*Ganoderma* sp.	*Phlebia brevispora*
Gene length (median), bp	1424	1541	1347
Transcript length (median), bp	1168	1182	1058
Protein length (median), aa	334	355	329
Exon length (median), bp	153	148	140
Intron length (median)	55	62	57
Exons per gene (median)	4	5	4

TABLE IV. EST and protein similarity support for the predicted genes in the three new Polyporales

	Bjerkandera adusta		*Ganoderma* sp.		*Phlebia brevispora*	
	Number	Percent	Number	Percent	Number	Percent
Total number of genes supported by:	15 473	100.00%	12 910	100.00%	16 170	100.00%
Homologs from Swissprot	8252	53.33%	7857	60.86%	9066	56.07%
Homologs from NCBI NR	11 166	72.16%	10 411	80.64%	12 604	77.95%
Predicted Pfam domain	6788	43.87%	6508	50.41%	7283	45.04%
EST alignment (>75%)	11 978	77.41%	10 553	81.74%	10 128	62.63%

acid identity of 76%, 7289 of them in syntenic regions (SUPPLEMENTARY TABLES III–V). Average identity between orthologs is 60–76% (SUPPLEMENTARY TABLE IV). The number of orthologs within Polyporales pairs can be as low as 5387 (*G. subvermispora-P. chrysosporium*; SUPPLEMENTARY TABLE III), which is comparable to the most distant pairs between Polyporales and Hymenochaetales (SUPPLEMENTARY TABLE V; 5382 in *F. mediterranea-G. subvermispora*, 5167 in *F. mediterranea-P. chrysosporium*). However, the number of syntenic orthologs is twice as high even in the most distant pair of Polyporales (3229 in *G. subvermispora-P. chrysosporium*) than between the groups (1764 in *F. mediterranea-P. chrysosporium*). The latter however depends on quality of assembly and may be lower for highly fragmented assemblies like *F. mediterranea*.

There is also synteny between multiple genomes. The largest group of 65 orthologous families (i.e. 15-member gene family, all of which have best hit of other) reside on the same scaffolds in 15 genomes, encompassing in average 1.2 Mb (max 2.5 Mb, min 0.55 Mb). In addition, 81 pairs of adjacent genes conserved in all 15 genomes.

While the details of the functional gene content were described in depth in companion papers (Ruiz-Dueñas et al. this issue), PFAM domain composition is comparable among all 10 Polyporales (SUPPLEMENTARY TABLES VI, VII). The top PFAM domains include p450, WD40 putatively involved protein-protein interaction, protein kinases involved in signaling, followed by transporters and other functions (SUPPLEMENTARY TABLE VI). HET domain has significant variation in Basidiomycota, often absent but significantly expanded in Polyporales *D. squalens* (112), *Ganoderma* sp. (90) and *Trametes versicolor* (159). PFAM domains, where at least one largest count is from Polyporales (SUPPLEMENTARY TABLE VII), include HET, hydrolases, Fe2 oxidases, iron reductases and others.

To go beyond functionally characterized protein domains, using MCL we clustered 129 895 proteins

TABLE V. Characterization of the new genomes according to the EuKaryotic orthologous groups (KOG) and the Kyoto Encyclopedia of Genes and Genomes (KEGG)

	B. adusta	*Ganoderma* sp.	*P. brevispora*
Total gene models	15 473	12 910	16 170
KOG: cellular processes and signaling	2731	2445	2855
KOG: information storage and processing	1790	1623	1871
KOG: metabolism	2322	2323	2765
KOG: poorly characterized	1676	1559	1792
KEGG: amino acid metabolism	588	581	615
KEGG: biosynthesis of polyketides and nonribosomal peptides	153	146	142
KEGG: biosynthesis of secondary metabolites	327	348	399
KEGG: carbohydrate metabolism	598	643	640
KEGG: energy metabolism	142	133	146
KEGG: glycan biosynthesis and metabolism	245	245	268
KEGG: lipid metabolism	534	546	585
KEGG: metabolism of cofactors and vitamins	465	457	519
KEGG: metabolism of other amino acids	131	127	132
KEGG: nucleotide metabolism	302	291	390
KEGG: overview	372	384	418
KEGG: xenobiotics biodegradation and metabolism	399	425	448

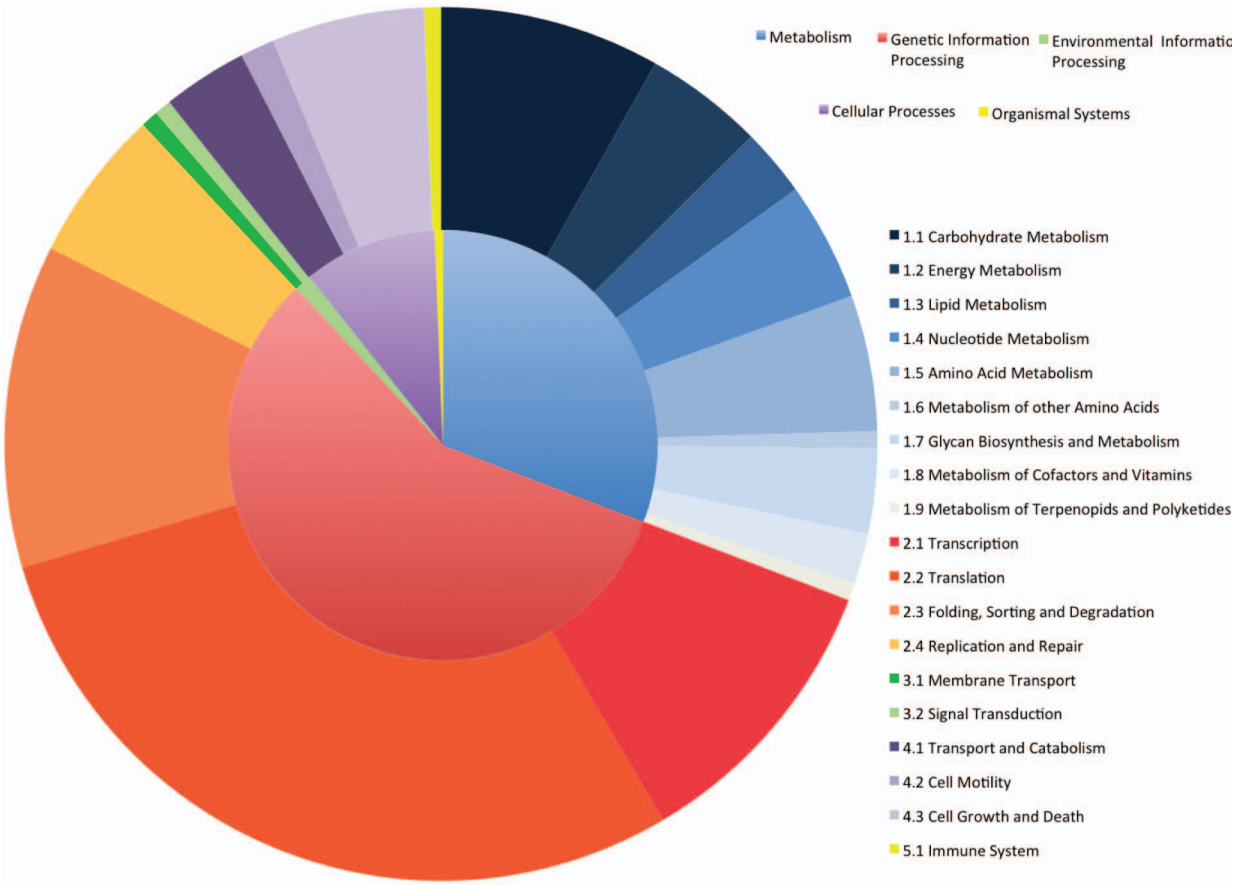

FIG. 1. Graphical overview of functions of single-copy present in the 10 Polyporales genomes according to the KOG classification.

from 10 Polyporales into 11 499 multigene groups and 9424 singletons. The core Polyporales set included 1776 clusters composed of 44 010 proteins from all 10 genomes, 534 of which contain exactly one member from each cluster.

Single-copy genes in Polyporales.—We identified 534 single-copy genes in the cluster including the 10 Polyporales genomes. The putative orthologs in yeasts and the higher functions of the genes are summarized (SUPPLEMENTARY FILE 1, FIG. 1). Higher-level functions could be predicted for only 159 out the 534 genes. For the phylogenomic and informativeness profiling analyses we selected a subset of 356 single-copy genes that were present in Polyporales and the outgroup taxa.

Phylogenomic analyses.—The 356-gene and 71-gene datasets have 145 050 and 44 385 amino acid positions respectively (gaps included). The resulting trees from the ML and BY analyses of both datasets have identical topologies (FIG. 2). In the 356-gene trees all internal nodes of the Polyporales receive 100% RaxML bootstrap support. In the 71-gene trees all nodes receive full support (100% RaxML bootstrap and a PhyloBayes posterior probability of 1.0 except the sister taxa relationship between *Gelatoporia subvermispora* and the antrodia clade (89% BS, 1.0 PP) and the sister taxa relationship between *Rhodonia placenta* and *Wolfiporia cocos* (92% BS and 1.0 PP). Support values for all nodes are provided (FIG. 2).

Informativeness profiling.—The 25 best performing genes in the phylogenetic informativeness profiling are provided (FIG. 3), together with the three AFTOL1 protein-coding genes (*rpb1*, *rpb2*, *tef1*). Information about these 25 genes is summarized (TABLE VI). Note that gene IDs refer to the Mycocosm cluster 1263 (Polyporales + outgroups) that unfortunately is no longer available. The nucleotide and protein sequences of all 356 genes profiled can be retrieved at wordpress.clarku.edu/polypeet/datasets/.

The resulting trees from the phylogenetic analyses of the 25-gene dataset (not shown) have an identical topology to the 356-gene and the 71-gene analyses (FIG. 2). All internal nodes of the Polyporales received full support (100% BS, 1 PP).

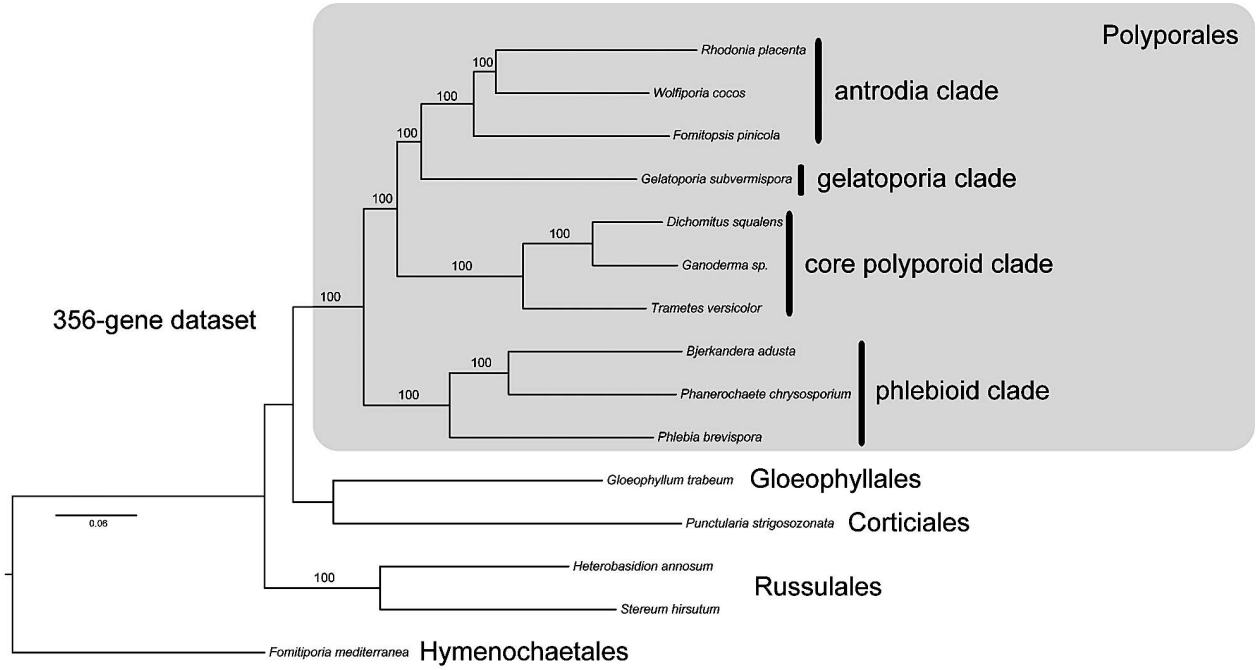

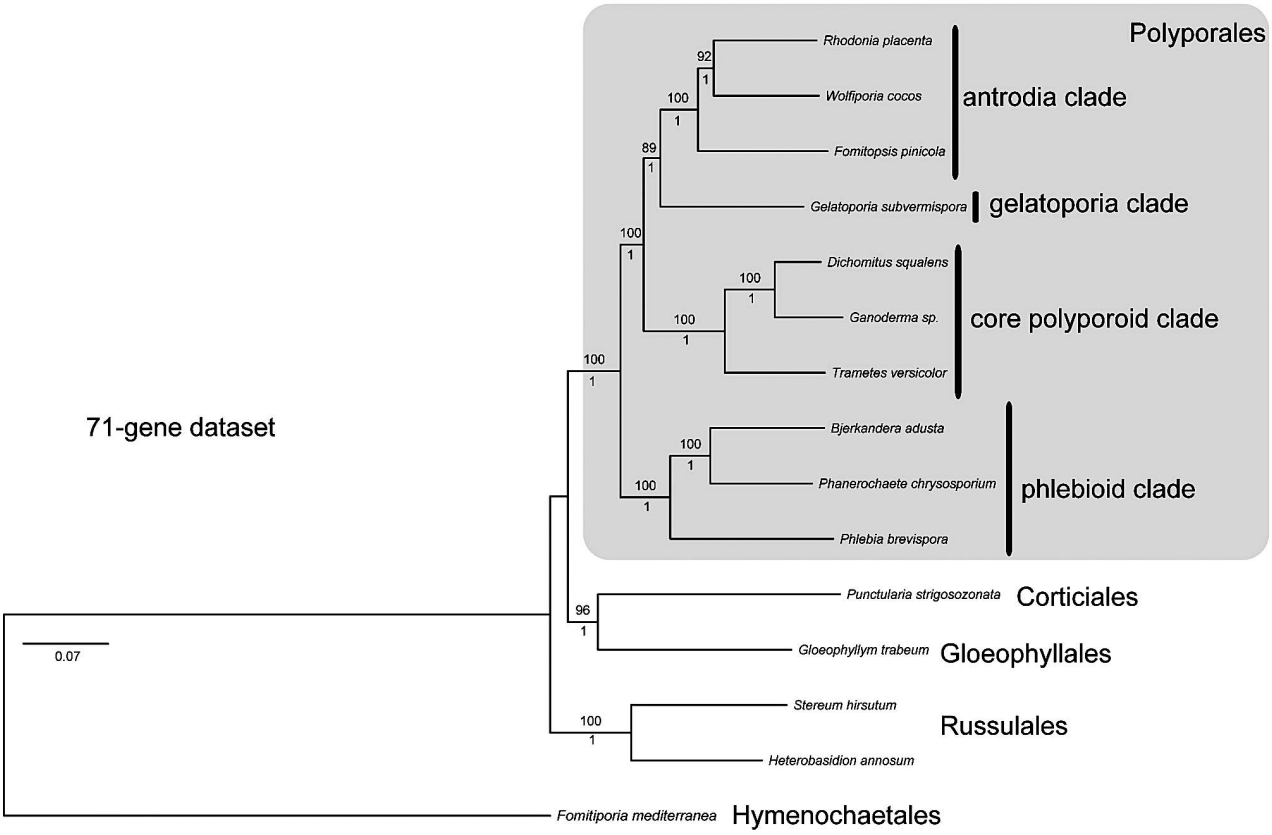

FIG. 2. Best trees from the ML analyses of the 356- and 71-gene datasets.

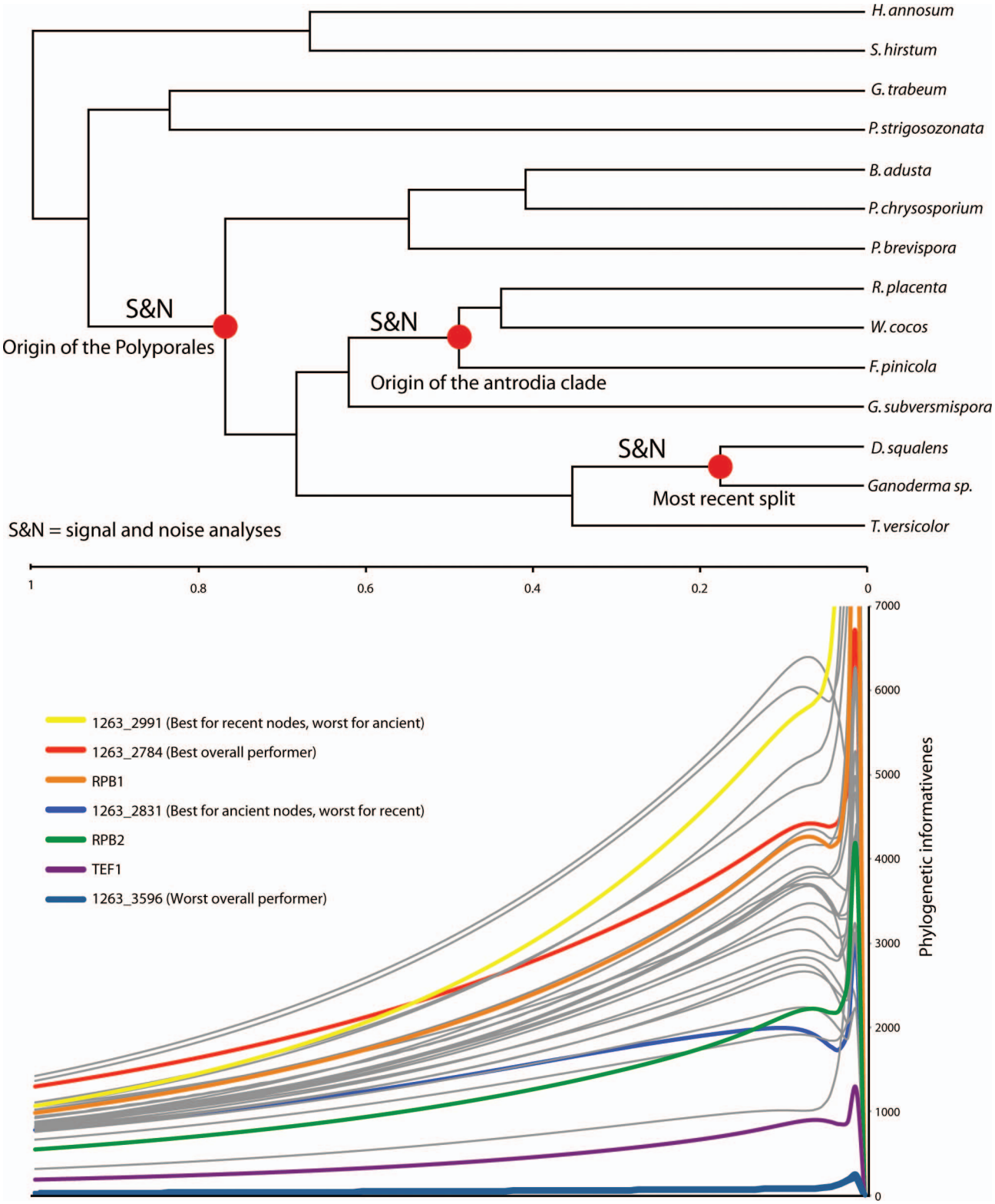

FIG. 3. Graphical overview of the phylogenetic informativeness of the 25 top candidate genes.

TABLE VI. Top 25 genes from the phylogenetic informativeness profiling analysis

Cluster 1263 ID	Nucleotide alignment	Putative yeast ortholog	Description
1263_2751	6946	SEN1	Presumed helicase required for RNA polymerase II transcription termination and processing of RNAs; homolog of Senataxin which causes Ataxia-Oculomotor Apraxia 2 and a dominant form of amyotrophic lateral sclerosis
1263_2765	7073	SWR1	Swi2/Snf2-related ATPase that is the structural component of the SWR1 complex, which exchanges histone variant H2AZ (Htz1p) for chromatin-bound histone
1263_2784	7400	unknown	Signaling protein DOCK180
1263_2789	4720	RRP5	RNA binding protein with preference for single stranded tracts of U's involved in synthesis of both 18S and 5.8S rRNAs; component of both the ribosomal small subunit (SSU) processosome and the 90S preribosome
1263_2790	5057	unknown6	Kinesin-like protein
1263_2794	5690	unknown5 (UBR1 like)	UBR1, related to ubiquitin-protein ligase e3 component
1263_2798	5586	unknown8 (VPS15 like)	VPS15-like, Serine/threonine protein kinase containing WD40 repeats
1263_2799	6110	MON2	Peripheral membrane protein with a role in endocytosis and vacuole integrity, interacts with Arl1p and localizes to the endosome; member of the Sec7p family of proteins
1263_2800	5374	POL1	Catalytic subunit of the DNA polymerase I alpha-primase complex, required for the initiation of DNA replication during mitotic DNA synthesis and premeiotic DNA synthesis
1263_2801	4752	YOR296W	Putative protein of unknown function; green fluorescent protein (GFP)-fusion protein localizes to the cytoplasm; expressed during copper starvation
1263_2802	4392	NCR1	Vacuolar membrane protein that transits through the biosynthetic vacuolar protein sorting pathway, involved in sphingolipid metabolism; glycoprotein and functional orthologue of human Niemann Pick C1 (NPC1) protein
1263_2806	6198	DOP1	Golgi-localized, leucine-zipper domain containing protein; involved in endosome to Golgi transport, organization of the ER, establishing cell polarity and morphogenesis; detected in highly purified mitochondria in high-throughput studies
1263_2810	3686	AMS1	Vacuolar alpha mannosidase, involved in free oligosaccharide (fOS) degradation; delivered to the vacuole in a novel pathway separate from the secretory pathway
1263_2817	7230	unknown9	Hypothetical protein
1263_2822	4917	RAV1	Subunit of the RAVE complex (Rav1p, Rav2p, Skp1p), which promotes assembly of the V-ATPase holoenzyme; required for transport between the early and late endosome/PVC and for localization of TGN membrane proteins; potential Cdc28p substrate
1263_2831	4140	SCP160	Essential RNA-binding G protein effector of mating response pathway, mainly associated with nuclear envelope and ER, interacts in mRNA-dependent manner with translating ribosomes via multiple KH domains, similar to vertebrate vigilins
1263_2840	5586	TRS120	One of 10 subunits of the transport protein particle (TRAPP) complex of the cis-Golgi which mediates vesicle docking and fusion; involved in endoplasmic reticulum (ER) to Golgi membrane traffic
1263_2843	4207	SEC8	Essential 121kDa subunit of the exocyst complex (Sec3p, Sec5p, Sec6p, Sec8p, Sec10p, Sec15p, Exo70p, and Exo84p), which has the essential function of mediating polarized targeting of secretory vesicles to active sites of exocytosis

TABLE VI. Continued

Cluster 1263 ID	Nucleotide alignment	Putative yeast ortholog	Description
1263_2856	4722	SKI3	Ski complex component and TPR protein, mediates 3′–5′ RNA degradation by the cytoplasmic exosome; null mutants have superkiller phenotype of increased viral dsRNAs and are synthetic lethal with mutations in 5′–3′ mRNA decay
1263_2902	4404	PDS5	Protein required for establishment and maintenance of sister chromatid condensation and cohesion, co-localizes with cohesin on chromosomes, may function as a protein-protein interaction scaffold; also required during meiosis
1263_2991	7954	SSM4	Ubiquitin-protein ligase involved in ER-associated protein degradation; located in the ER/nuclear envelope; ssm4 mutation suppresses mRNA instability caused by an rna14 mutation
1263_2996	4453	SRO77	Protein with roles in exocytosis and cation homeostasis; functions in docking and fusion of post-Golgi vesicles with plasma membrane; homolog of Sro7p and Drosophila lethal giant larvae tumor suppressor; interacts with SNARE protein Sec9p
1263_3045	6185	unknown51	Hypothetical protein
1263_3046	2822	unknown157	Hypothetical protein
1263_3047	4004	unknown19	Hypothetical protein

Multigene phylogenetic overview of the Polyporales.—The resulting trees from the maximum likelihood analyses, extended supermatrix (FIG. 4) and core supermatrix (FIG. 5), present essentially the same topology. The four major lineages of Polyporales recognized by Binder et al. (2005) are present in our analyses but only the core polyporoid and phlebioid clades appear well supported in both datasets. The composition and support of the antrodia and residual polyporoid clades and the status of some of the smaller lineages (tyromyces clade, gelatoporia clade, *Grifola*) remains unresolved (see DISCUSSION). The nodes that define the antrodia, core polyporoid, gelatoporia and phlebioid clade in the phylogenomic analyses (FIG. 2) are represented by equivalent nodes in the extended and core supermatrix analyses although with varying support. The tyromyces clade (not represented by genomic data) appears nested within the antrodia clade in the multigene analyses (see DISCUSSION). Except for the internal relations between the members of the antrodia clade, the individual taxa relationships obtained in the phylogenomic datasets (FIG. 2) also are reflected in the multigene datasets (FIGS. 4, 5). Throughout the paper clade names are written with no caps and no italics (e.g. antrodia clade) to avoid confusion with formal taxonomic names. Alignments haven been deposited in TreeBase under study number 13783. Supplementary analyses of ribosomal genes vs. protein-coding genes did not reveal any supported conflict between genes. These supplementary analyses and trees also can be retrieved from TreeBase. Phylogenetic and taxonomic implications of the multigene analyses are discussed below.

DISCUSSION

More genes or more taxa?—The increased availability of genome-scale data for Fungi has transformed mycology by opening a new universe of potential target genes to address ecological and systematical questions. Resolving the evolution of genes or gene families of enzymes involved in wood decay is of particular interest and will lead to a better characterization of the major wood-decay modes (Floudas et al. 2012). The number of published Polyporales genomes is limited currently to three brown-rot producing and seven white-rot producing species, and still the amount of data permits comparative work between and within ecological traits. Our previous view of functional boundaries within brown- and white-rot ecology clearly has been affected by the morphology of wood decay. However recent studies (e.g. Fernandez-Fueyo et al. 2012) suggest that upon genome analysis white-rot wood decay in the Polyporales generally may represent ecological variations of adaptations to substrates and colonization succession series, which would make the enzymes involved scalable for industrial applications.

We have identified 534 putative single-copy orthologs in 10 genomes of Polyporales (SUPPLEMENTARY FILE 1) and a subset of 356 genes also is shared by Corticiales, Gloeophyllales, Russulales and Hymenochaetales (FIG. 2). Many of these genes are poorly

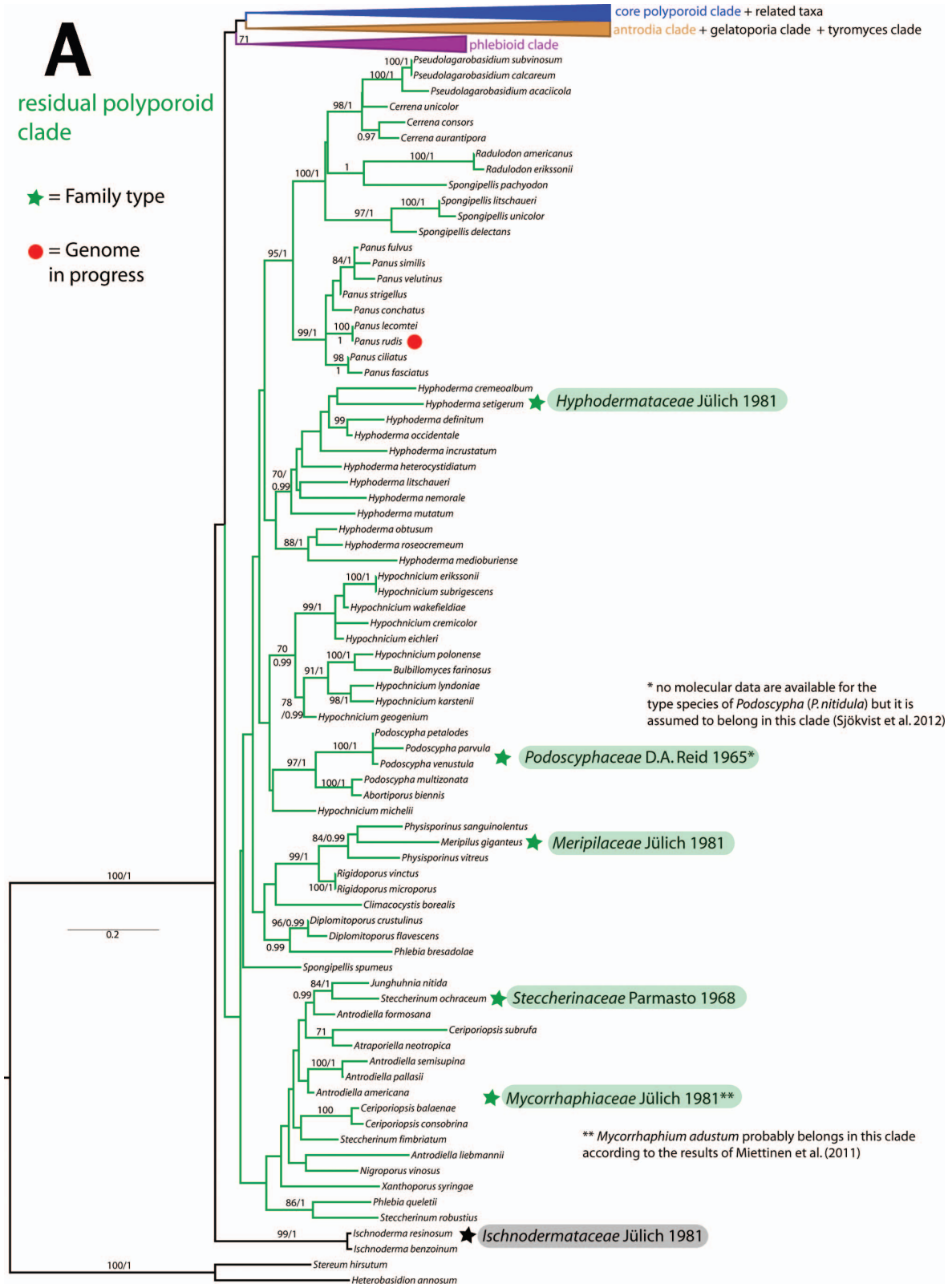

FIG. 4. A–D. Best tree from the ML analyses of the extended supermatrix dataset. Support values are on or below the branches. A. Residual polyporoid clade. B. Phlebioid clade. C. Core polyporoid clade. D. Antrodia clade.

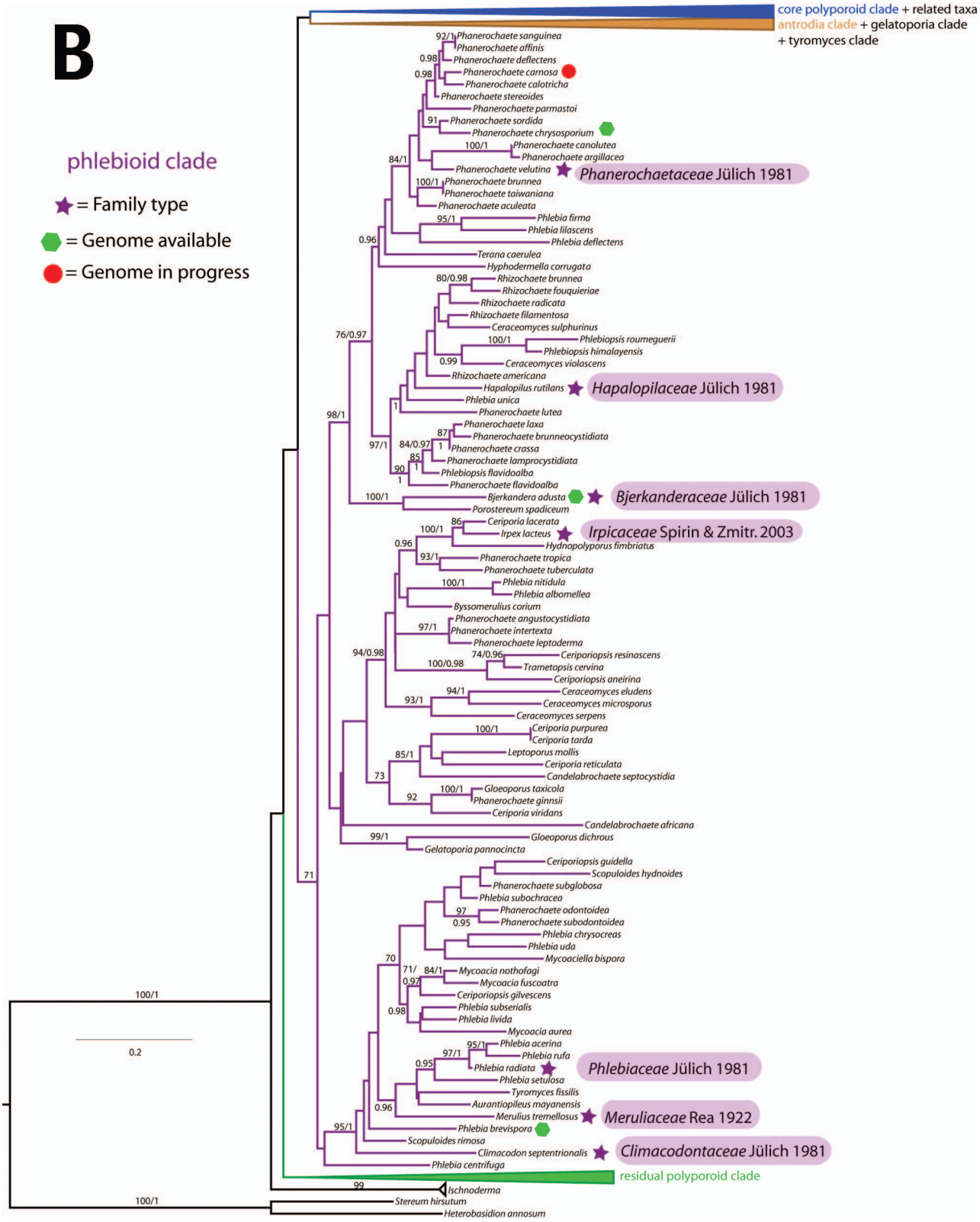

FIG. 4. Continued.

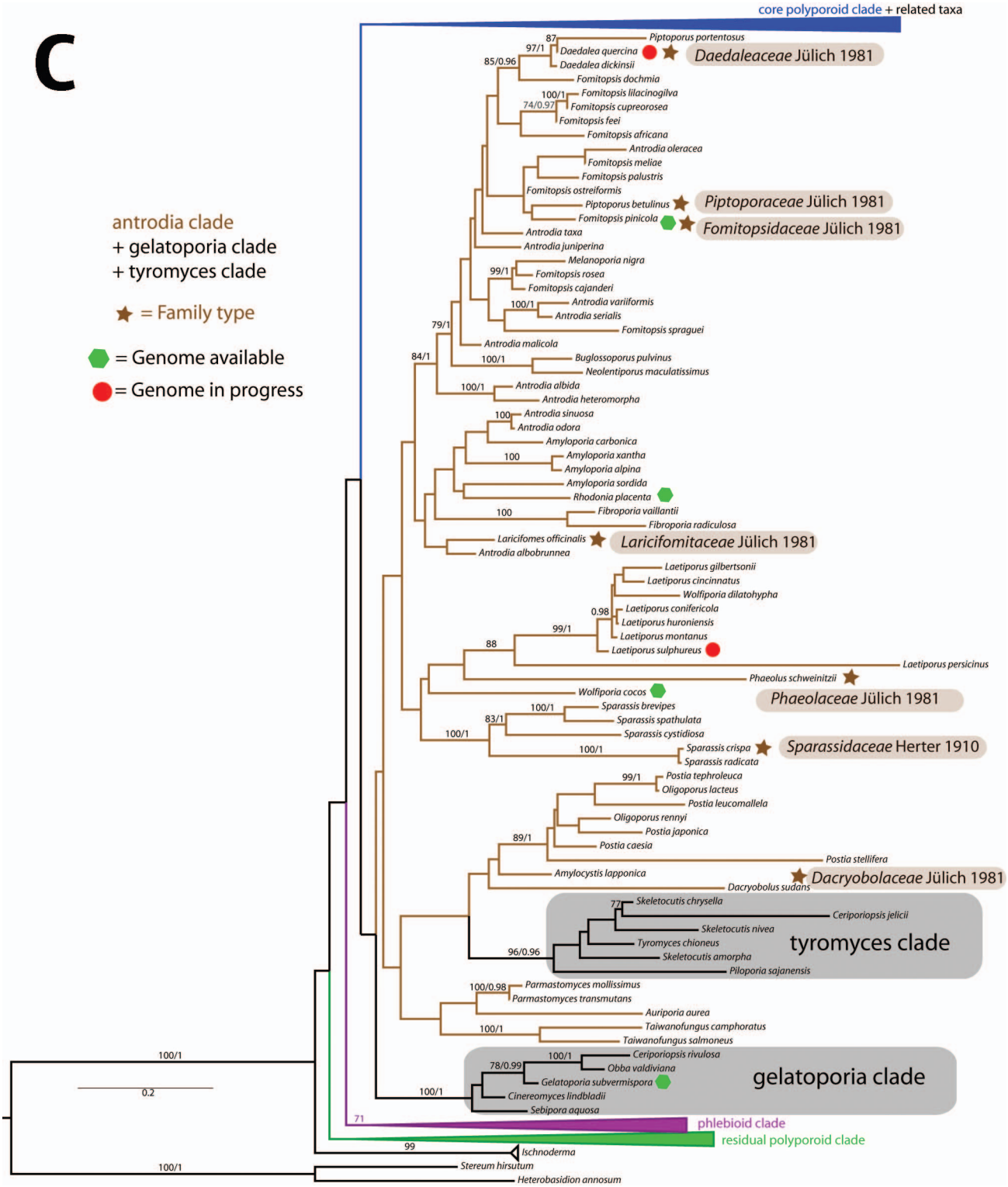

FIG. 4. Continued.

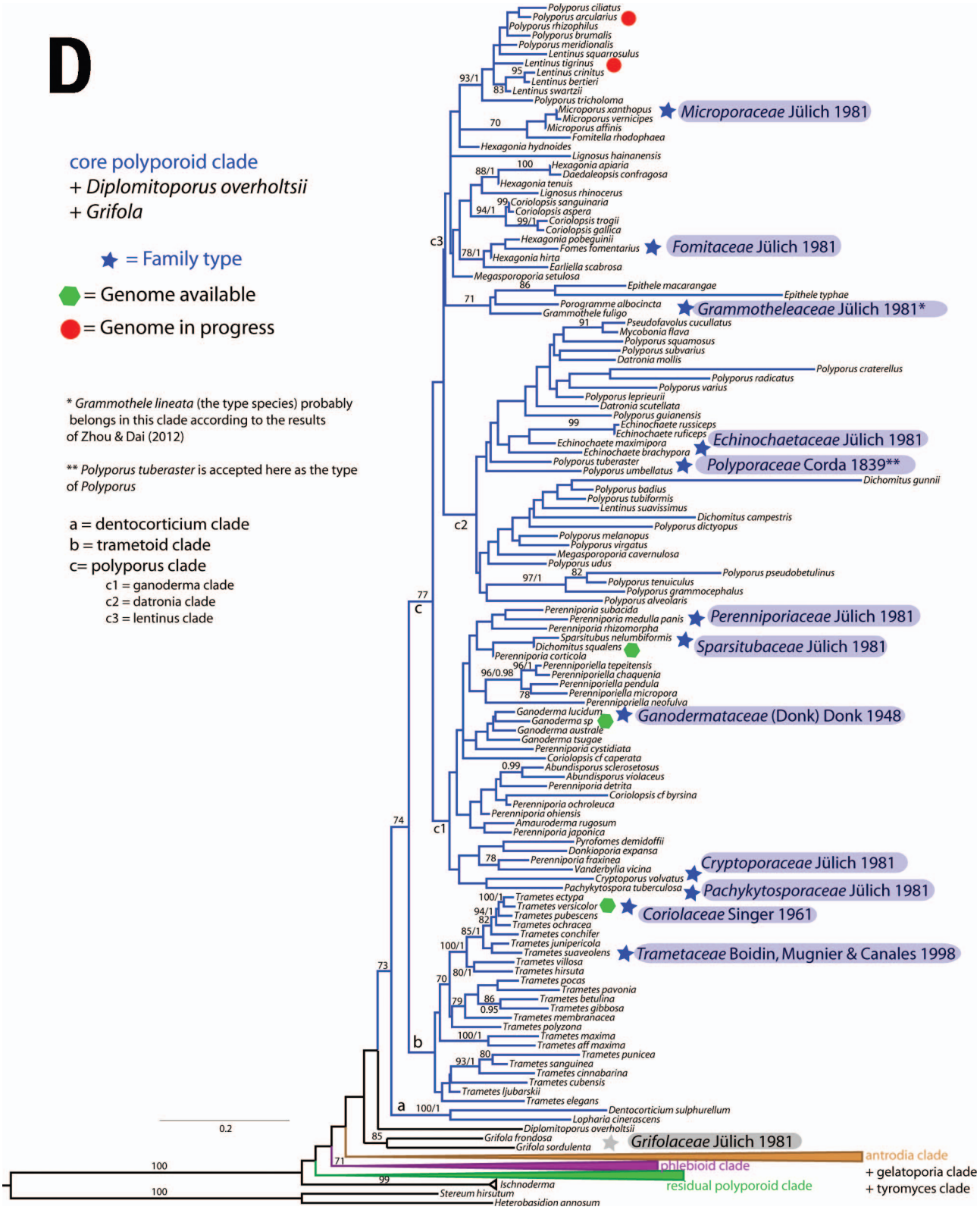

FIG. 4. Continued.

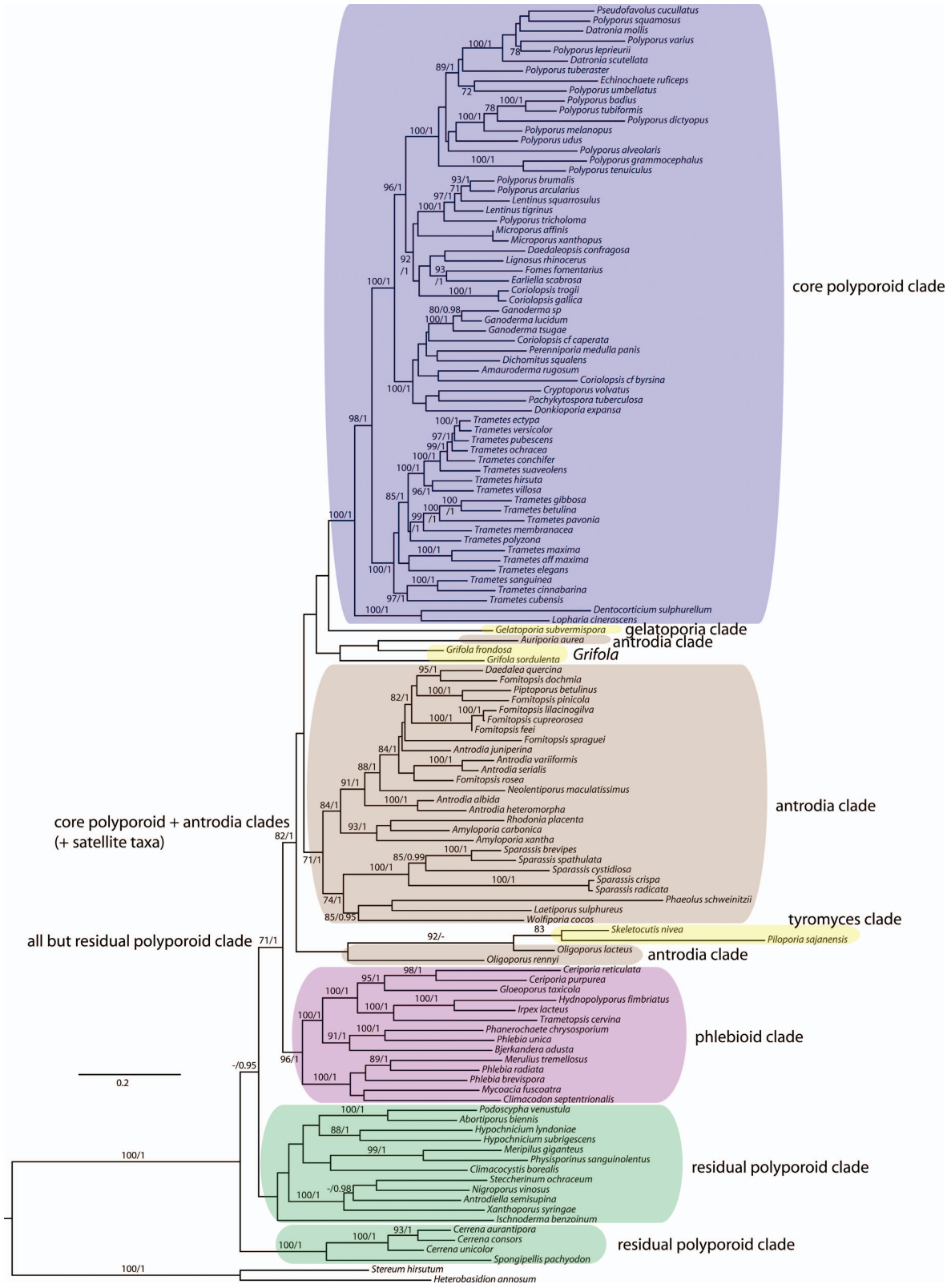

FIG. 5. Best tree from the ML analyses of the core supermatrix dataset. Support values are on or below branches.

characterized and labeled with ''unknown function'' or ''hypothetical protein'', and we only were able to assign 29% to higher level KEGG pathways (FIG. 1). The mechanisms and constraints for the maintenance of single-copy genes is not completely understood and their evolutionary rates can differ considerably, which may lead to topological incongruence (Wapinski et al. 2007, Feau et al. 2011). Nevertheless, single-copy genes hold great potential to improve phylogenetic resolution in clades that remain difficult based on analyses of commonly used universal loci (Aguileta et al. 2008). The most popular nonribosomal loci include *TEF1*, calmodulin, chitin synthase I, γ-actin (Carbone and Kohn 1999, Rehner and Buckley 2005), *atp6* (Kretzer and Bruns 1999), *RPB2* (Liu et al. 1999), *RPB1* (Matheny et al. 2002), β-tubulin and GPDH (Glass and Donaldson 1995). As illustrated in Feau et al. (2011), the use of these genes, individually or in combination, is disparate among studies and the resulting datasets are rarely overlap between the major fungal groups. From lessons learned we cannot expect to find a magic bullet that solves all our problems. In an attempt to answer the original question, ''more genes or more taxa?'', Rokas and Carroll (2005) concluded by making inferences from a dataset of 14 yeast genomes that the number of genes used is more important than the number of species. A denser sampling of larger, identical sets of genes has great potential to improve phylogenetic resolution and support (FIG. 2). In the present study we have shown that analyses of a (nearly complete) core dataset of Polyporales (FIG. 5) produce a better supported tree topology than in previous studies (e.g. Binder et al. 2005), which used four genes (nuclear and mitochondrial large and small subunits) and sampled ca. 125 Polyporales taxa (with only 47 represented by all four genes), and while the major groups discussed here were already apparent in that study there was no statistical support for any of them or for the relationships between them, only some nodes within those lineages received statistical support (cf. Binder et al. 2005 FIG. 4).

The phylogenetic trees presented here now can be used to select target species for the next round of whole genome sequencing. Our results from the extended core dataset (FIG. 4) also suggest that the introduction of missing data has its limitations and cannot be continued arbitrarily because it affects statistical support. Phylogenomics and phylogenetics are synergistic disciplines and the newly generated data will help build a robust backbone tree for the Polyporales.

We were able to reconstruct a fully resolved tree inferred from 25 out of 356 proteins identified through phylogenetic informativeness profiling (FIG. 3) (López-Giráldez and Townsend 2011), which will warrant further investigation in Polyporales and their allies. One option is individual primer design for the best performing genes, but this is a labor-intense, time-consuming process and there is no guarantee of finding a sufficient number of conservative sites to effectively cover larger parts of the genes. In addition, a broader applicability of newly designed primers has to stand the test of time and promising candidate genes, for example *FG1093* and *MS204* (Walker et al. 2012) or *mcm7* and *tsr1* (Schmitt et al. 2009), are still not widely used. Non PCR-based technologies are quickly advancing and offer an alternative to primer design (Faircloth et al. 2012, Lemmon et al. 2012). These methods use targeted hybrid DNA enrichment that makes it possible to analyze more than 500 genes simultaneously, which is roughly the size of the single-copy gene data for Polyporales, for up to 100 species. The objective is to identify conserved areas flanked by more variable regions in single-copy genes in small datasets of well studied genomes that serve as target probes. The probes then are tiled in small increments across the loci and combined across a species to generate a single probe set (Faircloth et al. 2012, Lemmon et al. 2012). This procedure has the advantage in that once a set of probes is produced, tiling permits its application to more distantly related species and libraries that have been constructed from the probe set can be subjected to high-throughput sequencing (Lemmon et al. 2012). Hybrid enrichment methods have the potential to tip the scales in favor of investigating more genes and more taxa in the imminent future.

Informativeness profiling.—All nodes of interest in the phylogeny are more ancient than the peaks of all of the informativeness profiles, so noise cannot be ignored and as a quantitative measure of utility the signal and noise-base probability of resolution should be used. The probabilities of resolution at each node of interest for all single-copy genes (SUPPLEMENTARY FILE 2) were used to sort genes by best performance across all epochs (FIG. 3). The overall best performer was 1263_2784; the overall worst was 1263_3596; the best performing for resolving recent nodes yet worst for ancient was 1263_2991 (ranked 18th overall); and the best performing for resolving ancient nodes yet worst for recent was 1263_2831 (ranked 9th overall).

It is worth noting the comparison between 1263_2991 and 1263_2831 because a cursory look at the informativeness profiles (FIG. 3) might give the impression that 1263_2991 would be better (it is always higher across the time scale plotted), but signal and noise tells us that is not so: noise from the high early peak makes it a poor subject for ancient resolution, whereas 1263_2831 is good at ancient

resolution, and despite being the biggest changer in the other direction it is a better overall choice because it still has sufficient information to resolve early nodes with some confidence.

The three AFTOL1 protein-coding genes, *rpb1*, *rpb2* and *tef1*, ranked 8th, 71st and 270th respectively (FIG. 3) in their overall phylogenetic resolution. Despite the great resolution power of *rpb1* across the epochs, it is by far the worst represented gene in GenBank with only 44 sequences of Polyporales available for this study.

Taxonomy of the Polyporales.—Our discussion centers around the major lineages recognized in the analyses of the extended supermatrix, core supermatrix and/or the phylogenomic datasets, the possible correspondence of those lineages with available family names in the Polyporales (TABLE I) and the recognition of critical nodes in the Polyporales phylogeny that need further attention. During the analyses it became evident that sets of sequences deposited in GenBank under different homotypic synonyms (e.g. *Phlebia deflectens*/*Phanerochete deflectens*; *Phanerochete flavidoalba*/*Phlebiopsis flavidoalba*) actually represent different species and that some taxa listed under different names (e.g. *Ischoderma benzoinum*/*Ischnoderma resinosum*; *Panus rudis*/*Panus lecomtei*) in fact might be the same species, however these species taxonomic problems are beyond the scope of the present study.

Residual polyporoid clade. Representative genera: *Abortiporus, Antrodiella, Atraporiella, Bulbillomyces, Cerrena, Climacocystis, Diplomitoporus, Hyphoderma, Hypochnicium, Ischnoderma, Junghuhnia, Meripilus, Nigroporus, Panus, Physisporinus, Podoscypha, Pseudolagarobasidium, Radulodon, Spongipellis, Steccherinum, Xanthoporus.* (The monophyly of many genera of the Polyporales mentioned in the discussion remains uncertain).

The name ''residual polypores'' was used first by Binder et al. (2005) to refer to a heterogeneous group of Polyporales that did not belong in any of the other lineages recognized by the authors (antrodia, core polyporoid and phlebioid clades). While the name is a practical way to refer to this group the monophyly of this lineage as a whole has yet to be proven. In our extended supermatrix tree *Ischnoderma* is placed as sister to all other Polyporales, and in the core supermatrix tree *Cerrena* and *Spongipellis* occupy that position. In both cases neither the placement of these taxa nor the grouping of the remainder residual polypores receives significant statistical support. In the core supermatrix tree (FIG. 5) the grouping of all Polyporales other than the residual polypores receives moderate to high statistical support (71% BS, 1 PP; FIG. 4A).

This group morphologically is extremely diverse including pileate-stipitate forms with gilled (*Panus*) or poroid hymenium (*Xanthoporus*), pileate-sessile (*Cerrena*), corticioid forms with smooth hymenium (*Hyphoderma*), stipitate-stereoid taxa (*Podoscypha*), resupinate-hydnoid (*Steccherinum*), resupinate-poroid (*Ceriporiopsis*) etc. The variation in microscopic characters is equally great with mono-, di- and trimitic taxa, clamp connections present or absent, cystidia present or absent etc. All taxa, however, are known to produce a white-rot wood decay (Ryvarden 1990, Bernicchia 2005, Bernicchia and Gorjón 2010).

Other than the grouping of *Cerrena*, *Panus*, *Pseudolagarobasidum*, *Radulodon* and *Spongipellis* in one clade the relationships between genera in this group remain largely unresolved. If research resolves the residual polyporoid clade as a monophyletic group and if one single family name is to be used for it then the name *Podoscyphaceae* is the oldest available. If several families are recognized for this lineage(s) there are at least five other available family names (FIG. 4A, TABLE I).

Resolving the phylogenetic relationships in this group is critical for identifying the earliest-diverging lineages in the Polyporales that eventually will allow for a detailed study of character evolution in the order. Unfortunately at present no genomic data for members of the residual polyporoid clade are available, but the genome sequencing of *Panus rudis* is in progress.

Phlebioid clade. Representative genera: *Aurantiopileus, Bjerkandera, Byssomerulius, Candelabrochaete, Ceriporia, Climacodon, Gloeoporus, Hapalopilus, Hydnopolyporus, Hyphodermella, Irpex, Leptoporus, Merulius, Mycoacia, Mycoaciella, Phanerochaete, Phlebia, Phlebiopsis, Porostereum, Rhizochaete, Scopuloides, Terana, Trametopsis.*

The term ''phlebioid clade'' first was introduced by Larsson et al. (2004) to refer to a group of corticioid and resupinate genera including *Phlebia*, *Byssomerulius* and *Hyphoderma* among others. Binder et al. (2005) maintained the use of the name but excluded from the phlebioid clade *Hyphoderma* and related taxa in that they were placed in the residual polyporoid clade, a result that is supported in the analyses presented here (FIG. 4B).

The phlebioid clade as defined here is only moderately supported in the extended supermatrix dataset (71% BS; FIG. 4B) but receives better support in the core supermatrix dataset (96% BS, 1 PP; FIG. 5) and also by the genomic dataset where *Bjerkandera adusta*, *Phanerochaete chrysosporium* and *Phlebia brevispora* are represented (FIG. 2). In all datasets the phlebioid clade is the sister group of the clade containing the antrodia and core polyporoid clades and their related lineages.

The taxonomy of many of the genera belonging in the phlebioid clade is far from settled, and a case in point example is the genus *Phlebia*. A total 26 taxa currently accepted in the genus *Phlebia*, including *Mycoacia*, *Mycoaciella* and *Merulius* (Nakasone and Burdsall 1984; Nakasone 1997, 2002; Bernicchia and Gorjón 2010; Moreno et al. 2011), were included in the extended supermatrix analyses, and they appear widely distributed in and out of the phlebioid clade; (i) *P. bresadolae* and *P. queletii* are placed in the residual polyporoid clade; (ii) the type species (*P. radiata*) groups with several *Phlebia*, *Merulius*, *Mycoacia* and *Mycoaciella* species, but taxa belonging to other genera (*Climacodon*, *Tyromyces*, *Scopuloides*, *Aurantiopileus*, *Ceriporiopsis* p.p.) appear intermixed with *Phlebia* species; (iii) *P. nitidula* and *P. albomellea* are more closely related to the lineage including *Ceraceomyces*, *Irpex* and *Trametopsis* than to other *Phlebia* species; (iv) *P. unica* appears in the same group as *Rhizochaete* and *Phlebiopsis*; (v) *P. deflectens*, *P. firma* and *P. lilascens* are closely related to *Phanerochaete*.

Corticioid and resupinate forms predominate in the phlebioid clade, but pileate forms also occur (e.g. *Hapalopilus*). There is an extensive variation in types of hymenium and microscopic characters. All taxa included in the phlebioid clade produce white-rot decay with one notable exception, *Leptoporus mollis*, which is placed in the extended dataset closely related to *Ceriporia*. *L. mollis* is described as causing a ''brown cubical rot on dead conifers'' (Gilbertson and Ryvarden 1986). The same authors wrote, ''The microscopic characters of *L. mollis* suggest relationships with species of *Ceriporia*, all white-rot fungi. Because *L. mollis* does not show close affinities to other brown-rot fungi it is best kept as a monotypic genus.'' The seemingly anomalous phylogenetic position of *Leptoporus* was noted by Lindner and Banik (2008) and, if confirmed in subsequent analyses, it would represent an independent origin of the brown-rot ecology in the Polyporales outside the antrodia clade.

The name *Meruliaceae* is the oldest available at the family level for the phlebioid clade. If several families are recognized in this lineage there are six other available family names (FIG. 4B, TABLE I). Three genomes currently are available for taxa in the phlebioid clade: *Bjerkandera adusta*, *Phlebia brevispora*, and *Phanerochaete chrysosporium* and the genome of *Phanerochaete carnosa* is currently in progress.

Antrodia clade, gelatoporia clade, tyromyces clade and Grifola. Representative genera: *Amylocystis*, *Amyloporia*, *Antrodia*, *Auriporia*, *Buglossoporus*, *Cinereomyces*, *Dacryobolus*, *Daedalea*, *Fibroporia*, *Fomitopsis*, *Gelatoporia*, *Grifola*, *Laetiporus*, *Laricifomes*, *Neolentiporus*, *Obba*, *Oligoporus*, *Parmastomyces*, *Phaeolus*, *Piloporia*, *Piptoporus*, *Postia*, *Rhodonia*, *Sebipora*, *Skeletocutis*, *Sparassis*, *Taiwanofungus*, *Tyromyces*, *Wolfiporia*.

The antrodia clade was introduced first by Hibbett and Donoghue (2001) and further delineated by Binder et al. (2005). All taxa putatively belonging in the clade share brown-rot wood decay. The composition and support of the antrodia clade has been, and remains, one of the major issues in the phylogeny of the Polyporales. In the analyses by Binder et al. (2005) isolates of the white-rot *Climacocystis* sp., *Grifola frondosa* and (in some topologies) *Ischnoderma benzoinum* were nested inside the antrodia clade. In the analyses by Garcia-Sandoval et al. (2011) *Grifola frondosa* again was nested inside the antrodia clade.

In our extended supermatrix analysis none of these taxa appears nested in the antrodia clade but a small clade of white-rot polypores (the tyromyces clade, FIG. 4C) is nested within two brown-rot lineages. This placement receives no statistical support but brings to our attention this recurring problem and the need to clarify the phylogenetic position of the lineages that are not brown rot (antrodia clade); neither are supported as belonging in the core polyporoid clade (discussed below). Some of these lineages have been studied in detail by Miettinen and Rajchenberg (2012) who, based on nrLSU and ITS data, placed the gelatoporia clade (''*Cinereomyces* clade'' in their study) as the sister group of the core polyporoid clade and the tyromyces clade as sister to a clade containing the residual, phlebioid and antrodia clades plus *Grifola*. In our analyses the phylogenetic position of these lineages is not well resolved: (i) the gelatoporia clade is placed as the sister group of the antrodia clade + tyromyces clade (extended supermatrix, FIG. 4C) or as sister to the core polyporoid clade (core supermatrix, FIG. 5). In the genomic analyses *Gelatoporia subvermispora* is sister to the antrodia clade (FIG. 2); (ii) The tyromyces clade appears nested in the antrodia clade (extended supermatrix, FIG. 4C) or intermixed with *Oligoporus* species that cluster separately from the rest of the antrodia clade (core supermatrix, FIG. 5); (iii) *Grifola* appears as sister to the core polyporoid + *Diplomitoporus overholtsii* (extended supermatrix, FIG. 4D) or intermixed with *Auriporia aurea* and sister to the core polyporoid + gelatoporia clades (core supermatrix, FIG. 5).

The clade containing these satellite lineages plus the antrodia and core polyporoid clades is relatively well supported in the core-supermatrix dataset (82% BS, 1 PP; FIG. 5) and receives full support in the genomic analyses (FIG. 2). Resolving the internal relations among the lineages in this clade is critical for elucidating the origins of brown-rot polypores and how many transitions between white and brown rot

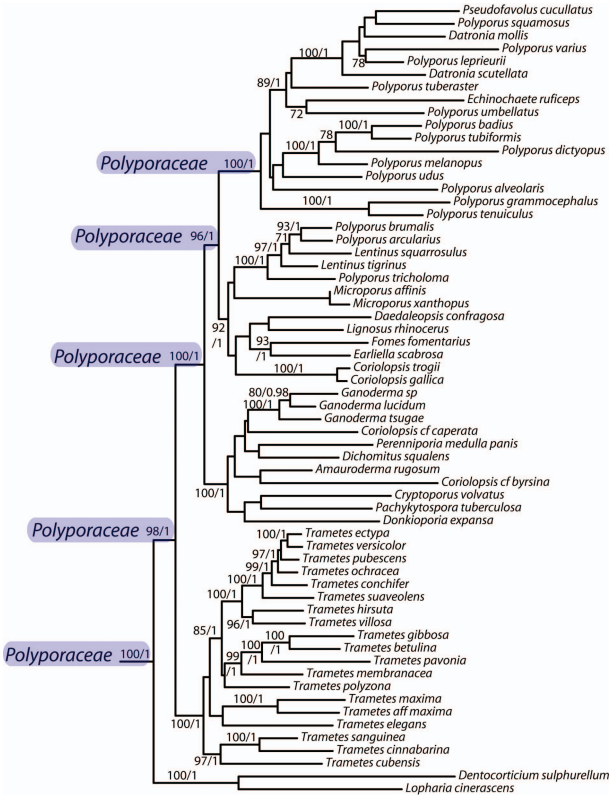

FIG. 6. Alternative circumscriptions of the *Polyporaceae* based on the results of the core supermatrix dataset.

have occurred in the Polyporales. Our results do not support the previously suggested reversal to white rot from brown rot for *Grifola* (García-Sandoval et al. 2011), but the unresolved position of these small white-rot lineages with respect to the brown-rot antrodia clade needs further study.

Pileate-stipitate (e.g. *Phaeolus*), pileate-sessile (e.g. *Oligoporus*) and resupinate forms (e.g. *Amylocystis*) with poroid hymenophores are predominant in the antrodia clade, but true corticioids with smooth hymenophores (e.g. *Dacryobolus*), taxa with daedaleoid hymenophores (*Daedalea*) and species with cauliflower-like basidiocarps (*Sparassis*) also exist. A detailed phylogenetic overview of the genus taxonomy of the antrodia clade is given by Ortiz-Santana et al. (this issue) Three genomes are available for taxa in the antrodia clade: *Fomitopsis pinicola*, *Rhodonia placenta* and *Wolfiporia cocos* and two more are in progress for *Daedalea quercina* and *Laetiporus sulphureus*.

If the antrodia clade is resolved as monophyletic and one family name is used for it, the name *Sparassidaceae* is the oldest available. If several families are recognized for this lineage(s), there are six other available family names (FIG. 4C). The name *Grifolaceae* is available for *Grifola* that apparently does not belong to either the antrodia or core polyporoid clades. No family names are available for the gelatoporia and tyromyces clades.

Core polyporoid clade. Representative genera: *Abundisporus*, *Amauroderma*, *Coriolopsis* sensu lato, *Cryptoporus*, *Datronia*, *Dichomitus*, *Donkioporia*, *Earliella*, *Echinochaete*, *Epithele*, *Fomes*, *Fomitella*, *Ganoderma*, *Grammothele*, *Hexagonia*, *Lentinus*, *Lignosus*, *Megasporoporia*, *Microporus*, *Pachykytospora*, *Perenniporia*, *Perenniporiella*, *Polyporus* sensu lato, *Porogramme*, *Pyrofomes*, *Sparsitubus*, *Trametes*, *Vanderbylia*.

The term ''core polyporoid clade'' was introduced first by Binder et al. (2005), although it was recognized under different names before that, for example ''polyporoid clade'' in Larsson et al. (2004), *Polyporaceae* in Kim and Jung (2000). The core polyporoid clade receives only moderate support in the extended supermatrix dataset (73% BS, FIG. 4C) and full support in the core supermatrix and genomic datasets (FIGS. 2, 5). The three major lineages of the core polyporoid clade recognized by Justo and Hibbett (2011) are present in the extended and core datasets (FIGS. 4D, 5), but they receive only significant support in the later: (i) dentocorticium clade. Includes *Dentocorticium sulphurellum* and *Lopharia cinerascens*. This is very likely the earliest diverging lineage in the core polyporoid clade; (ii) trametoid clade. Corresponds to *Trametes* in the sense of Justo and Hibbett (2011). Other authors (e.g. Welti et al. 2012) have proposed a different taxonomic organization for this clade; (iii) polyporus clade. The three lineages named by Justo and Hibbett (2011) as datronia clade, ganoderma clade and lentinus clade are present in the extended and core datasets, with good support values in the later.

Pileate-stipitate and pileate-sessile basidiocarps with poroid hymenophores are predominant in the core polyporoid clade, but taxa with lamellate hymenophores (e.g. *Lentinus*, *Trametes*) and resupinate forms (e.g. *Dentocorticium*, *Grammothele*) also exist. Most of the taxa have di- or trimitic hyphal systems and tetrapolar mating systems. All taxa in the core polyporoid clade produce a white-rot wood decay.

The use of the family name *Polyporaceae* perfectly exemplifies the need for a consensus among taxonomists for a formal suprageneric taxonomic arrangement in the Polyporales. Assuming that the phylogeny of the core polyporoid clade presented here is supported in future studies, five well supported nodes in the core polyporoid clade can define the limits of the *Polyporaceae* (FIG. 6). Three genomes are available for taxa in the core polyporoid clade, *Dichomitus squalens*, *Ganodema* sp. and *Trametes versicolor*, and two more are in progress for *Lentinus tigrinus* and *Polyporus arcularius*.

ACKNOWLEDGMENTS

We acknowledge the financial support of NSF through the PolyPEET grant (DEB 0933081) to DSH. The work conducted by the US Department of Energy Joint Genome Institute is supported by the Office of Science of the US Department of Energy under contract No. DE-AC02-05CH11231.

LITERATURE CITED

Aguilet G, Marthey S, Chiapello H, Lebrun M-H, Rodolphe F, Fournier E, Gendrault-Jacquemard A, Giraud T. 2008. Assessing the performance of single-copy genes for recovering robust phylogenies. Syst Biol 57:613–627, doi:10.1080/10635150802306527

Bernicchia A. 2005. Polyporaceae s.l. Fungi Europaei 10. Alassio: Ed. Candusso. 808 p.

———, Gorjon SP. 2010. Corticiaceae s.l. Fungi Europaei 12. Alassio: Ed. Candusso. 1008 p.

Binder M, Hibett DS, Larsson KH, Larsson E, Langer E, Langer G. 2005. The phylogenetic distribution of resupinate forms across the major clades of mushroom-forming fungi (homobasidiomycetes). Syst Biodivers 3:113–157, doi:10.1017/S1477200005001623

Carbone I, Kohn LM. 1999. A method for designing primer sets for speciation studies in filamentous Ascomycetes. Mycologia 91:553–556, doi:10.2307/3761358

Castresana J. 2000. Selection of conserved blocks from multiple alignments for their use in phylogenetic analysis. Mol Biol Evol 17:540–552, doi:10.1093/oxfordjournals.molbev.a026334

Chen S, Xu J, Liu C, Zhu Y, Nelson DR, Zhou S, Li C, Wang L, Guo X, Sun Y, Luo H, Li Y, Song J, Henrissat B, Levasseur A, Qian J, Li J, Luo X, Shi L, He L, Xiang L, Xu X, Niu Y, Li Q, Han MV, Yan H, Zhang J, Chen H, Lv A, Wang Z, Liu M, Schwartz DC, Sun C. 2012. Genome sequence of the model medicinal mushroom *Ganoderma lucidum*. Nat Commun 26:913, doi:10.1038/ncomms1923

Eastwood DC, Floudas D, Binder M, Majcherczyk A, Schneider P, Aerts A, Asiegbu FO, Baker SE, Barry K, Bendiksby M, Blumentritt M, Coutinho PM, Cullen D, de Vries RP, Gathman A, Goodell B, Henrissat B, Ihrmark K, Kauserud H, Kohler A, LaButti K, Lapidus A, Lavin JL, Lee YH, Lindquist E, Lilly W, Lucas S, Morin E, Murat C, Oguiza JA, Park J, Pisabarro AG, Riley R, Rosling A, Salamov A, Schmidt O, Schmutz J, Skrede I, Stenlid J, Wiebenga A, Xie X, Kües U, Hibbett DS, Hoffmeister D, Högberg N, Martin F, Grigoriev IV, Watkinson SC. 2011. The plant cell wall-decomposing machinery underlies the functional diversity of forest fungi. Science 333:762–765, doi:10.1126/science.1205411

Faircloth BC, McCormack JE, Crawford NG, Harvey MG, Brumfield RT, Glenn TC. 2012. Ultraconserved elements anchor thousands of genetic markers spanning multiple evolutionary timescales. Syst Biol 61:717–726, doi:10.1093/sysbio/sys004

Feau N, Decourcelle T, Husson C, Desprez-Loustau M-L, Dutech C. 2011. Finding single copy genes out of sequenced genomes for multilocus phylogenetics in non-model Fungi. PLoS ONE 6(4):e18803, doi:10.1371/journal.pone.0018803

Fernandez-Fueyo E, Ruiz-Dueñas FJ, Ferreira P, Floudas D, Hibbett DS, Canessa P, Larrondo LF, James TY, Seelenfreund D, Lobos S, Polanco R, Tello M, Honda Y, Watanabe T, Watanabe T, Ryu JS, Kubicek CP, Schmoll M, Gaskell J, Hammel KE, St John FJ, Vanden Wymelenberg A, Sabat G, Splinter BonDurant S, Syed K, Yadav JS, Doddapaneni H, Subramanian V, Lavín JL, Oguiza JA, Perez G, Pisabarro AG, Ramirez L, Santoyo F, Master E, Coutinho PM, Henrissat B, Lombard V, Magnuson JK, Kües U, Hori C, Igarashi K, Samejima M, Held BW, Barry KW, LaButti KM, Lapidus A, Lindquist EA, Lucas SM, Riley R, Salamov AA, Hoffmeister D, Schwenk D, Hadar Y, Yarden O, de Vries RP, Wiebenga A, Stenlid J, Eastwood D, Grigoriev IV, Berka RM, Blanchette RA, Kersten P, Martinez AT, Vicuna R, Cullen D. 2012. Comparative genomics of *Ceriporiopsis subvermispora* and *Phanerochaete chrysosporium* provide insight into selective ligninolysis. Proc Natl Acad Sci USA 109:5458–5463, doi:10.1073/pnas.1119912109

Floudas D, Binder M, Riley R, Barry K, Blanchette RA, Henrissat B, Martínez AT, Otillar R, Spatafora JW, Yadav JS, Aerts A, Benoit I, Boyd A, Carlson A, Copeland A, Coutinho PM, de Vries RP, Ferreira P, Findley K, Foster B, Gaskell J, Glotzer D, Górecki P, Heitman J, Hesse C, Hori C, Igarashi K, Jurgens JA, Kallen N, Kersten P, Kohler A, Kües U, Kumar TK, Kuo A, LaButti K, Larrondo LF, Lindquist E, Ling A, Lombard V, Lucas S, Lundell T, Martin R, McLaughlin DJ, Morgenstern I, Morin E, Murat C, Nagy LG, Nolan M, Ohm RA, Patyshakuliyeva A, Rokas A, Ruiz-Dueñas FJ, Sabat G, Salamov A, Samejima M, Schmutz J, Slot JC, St John F, Stenlid J, Sun H, Sun S, Syed K, Tsang A, Wiebenga A, Young D, Pisabarro A, Eastwood DC, Martin F, Cullen D, Grigoriev IV, Hibbett DS. 2012. The Paleozoic origin of enzymatic lignin decomposition reconstructed from 31 fungal genomes. Science 336:1715–1719, doi:10.1126/science.1221748

Garcia-Sandoval R, Wang Z, Binder M, Hibbett DS. 2011. Molecular phylogenetics of the Gloeophyllales and relative ages of clades of Agaricomycotina producing a brown rot. Mycologia 103:510–524, doi:10.3852/10-209

Gilbertson RL, Ryvarden L. 1986. North American polypores. Vol. 1. Synopsis Fungorum Special Volume. Oslo: Fungiflora. 433 p.

Glass NL, Donaldson GC. 1995. Primer sets developed to amplify conserved genes from filamentous Ascomycetes are useful in differentiating *Fusarium* species associated with conifers. Appl Environ Microbiol 61:1331–1340.

Grigoriev IV, Cullen D, Goodwin SB, Hibbett DS, Jeffries TW, Kubicek CP, Kuske C, Magnuson J, Martin F, Spatafora J, Tsang A, Baker S. 2011. Fueling the future with fungal genomics. Mycology 2:192–209.

———, Nordberg H, Shabalov I, Aerts A, Cantor M, Goodstein D, Kuo A, Minovitsky S, Nikitin R, Ohm RA, Otillar R, Poliakov A, Ratnere I, Riley R, Smirnova T, Rokhsar D, Dubchak I. 2012. The genome portal of the Department of Energy Joint Genome Institute.

Nucleic Acid Res 40(Database issue):D26–32, doi:10.1093/nar/gkr947

Guindon S. 2010. Bayesian estimation of divergence times from large sequence alignments. Mol Biol Evol 27: 1768–81, doi:10.1093/molbev/msq060

———, Gascuel O. 2003. A simple, fast and accurate algorithm to estimate large phylogenies by maximum likelihood. Syst Biol 52:696–704, doi:10.1080/10635150390235520

Hibbett DS. 2007. After the gold rush, or before the flood? Evolutionary morphology of mushroom-forming fungi (Agaricomycetes) in the early 21st century. Mycol Res. 111:1001–1018, doi:10.1016/j.mycres.2007.01.012

———, Donoghue MJ. 1995. Progress toward a phylogenetic classification of the Polyporaceae through parsimony analyses of ribosomal DNA sequences. Can J Bot 73(Suppl. 1):S853–S861, doi:10.1139/b95-331

———, ———. 2001. Analysis of character correlations among wood decay mechanisms, mating systems, and substrate ranges in homobasidiomycetes. Syst Biol 50: 215–42, doi:10.1080/10635150151125879

Jülich W. 1981. Higher taxa of basidiomycetes. Bibliothec Mycol 85:5–485.

Justo A, Hibbett DS. 2011. Phylogenetic classification of *Trametes* (Polyporales, Basidiomycota) based on a five-marker dataset. Taxon 60:1567–1583.

Katoh K, Kuma K, Toh H, Miyata T. 2005. MAFFT 5: improvement in accuracy of multiple sequence alignment. Nucleic Acids Res 33:511–8, doi:10.1093/nar/gki198

Kim SY, Jung HS. 2000. Phylogenetic relationships of the Aphyllophorales inferred from sequence analysis of nuclear small subunit ribosomal DNA. J Microbiol 38:122–131.

Kirk PM, Cannon PF, David JC, Minter DW, Stalpers JA. 2008. Ainsworth and Bisby's Dictionary of the Fungi. 10th ed. Wallingford, Oxon, UK: CAB International Press. 771 p.

Kretzer AM, Bruns TD. 1999. Use of atp6 in fungal phylogenetics: an example from the Boletales. Mol Phylogenet Evol 13:483–492, doi:10.1006/mpev.1999.0680

Krüger D, Gargas A. 2004. The basidiomycete genus Polyporus—an emendation based on phylogeny and putative secondary structure of ribosomal RNA molecules. Feddes Repertorium 115:503–546, doi:10.1002/fedr.200311052

Larsson KH. 2007. Re-thinking the classification of corticioid fungi. Mycol Res 111:1040–1063, doi:10.1016/j.mycres.2007.08.001

———, Larsson E, Kõljalg U. 2004. High phylogenetic diversity among corticioid homobasidiomycetes. Mycol Res 108:983–1002, doi:10.1017/S0953756204000851

Lartillot N, Lepage T, Blanquart S. 2009. PhyloBayes 3: a Bayesian software package for phylogenetic reconstruction and molecular dating. Bioinformatics 25:2286–2288, doi:10.1093/bioinformatics/btp368

Lemmon AR, Emme SA, Lemmon EM. 2012. Anchored hybrid enrichment for massively high-throughput phylogenomics. Syst Biol 61:727–744, doi:10.1093/sysbio/sys049

Lindner DL, Banik MT. 2008. Molecular phylogeny of *Laetiporus* and other brown-rot polypore genera in North America. Mycologia 100:417–30, doi:10.3852/07-124R2

Liu YJ, Wheelen S, Hall BD. 1999. Phylogenetic relationships among Ascomycetes: evidence from an RNA polymerase II subunit. Mol Biol Evol 16:1799–1808, doi:10.1093/oxfordjournals.molbev.a026092

López-Giráldez F, Townsend JP. 2011. PhyDesign: an online application for profiling phylogenetic informativeness. BMC Evol Biol 11:152, doi:10.1186/1471-2148-11-152

Matheny PB, Liu YJ, Ammirati JF, Hall BD. 2002. Using *RPB1* sequences to improve phylogenetic inference among mushrooms (*Inocybe*, Agaricales). Am J Bot 89: 688–698, doi:10.3732/ajb.89.4.688

Martinez D, Challacombe J, Morgenstern I, Hibbett D, Schmoll M, Kubicek CP, Ferreira P, Ruiz-Duenas FJ, Martinez AT, Kersten P, Hammel KE, Vanden Wymelenberg A, Gaskell J, Lindquist E, Sabat G, Bondurant SS, Larrondo LF, Canessa P, Vicuna R, Yadav J, Doddapaneni H, Subramanian V, Pisabarro AG, Lavín JL, Oguiza JA, Master E, Henrissat B, Coutinho PM, Harris P, Magnuson JK, Baker SE, Bruno K, Kenealy W, Hoegger PJ, Kües U, Ramaiya P, Lucas S, Salamov A, Shapiro H, Tu H, Chee CL, Misra M, Xie G, Teter S, Yaver D, James T, Mokrejs M, Pospisek M, Grigoriev IV, Brettin T, Rokhsar D, Berka R, Cullen D. 2009. Genome, transcriptome and secretome analysis of wood-decay fungus *Postia placenta* supports unique mechanisms of lignocellulose conversion. Proc Natl Acad Sci USA 106:1954–1959, doi:10.1073/pnas.0809575106

———, Larrondo LF, Putnam N, Gelpke MD, Huang K, Chapman J, Helfenbein KG, Ramaiya P, Detter JC, Larimer F, Coutinho PM, Henrissat B, Berka R, Cullen D, Rokhsar D. 2004. Genome sequence of the lignocellulose-degrading fungus *Phanerochaete chrysosporium* strain RP78. Nat Biotechnol. 22:695–700, doi:10.1038/nbt967

Mayrose I, Mitchell A, Pupko T. 2005. Site-specific evolutionary rate inference: taking phylogenetic uncertainty into account. J Mol Evol 60:345–53, doi:10.1007/s00239-004-0183-8

Miettinen O, Larsson E, Sjökvist E, Larsson KL. 2011. Comprehensive taxon sampling reveals unaccounted diversity and morphological plasticity in a group of dimitic polypores (Polyporales, Basidiomycota). Cladistics 28:251–7270, doi:10.1111/j.1096-0031.2011.00380.x

———, Rajchenberg M. 2012. Obba and Sebipora, new polypore genera related to *Cinereomyces* and *Gelatoporia* (Polyporales, Basidiomycota). Mycol. Prog 11:131–147, doi:10.1007/s11557-010-0736-8

Moreno G, Blanco MN, Checa J, Platas G, Peláez F. 2011. Taxonomic and phylogenetic revision of three rare irpicoid species within the Meruliaceae. Mycol Prog 10: 481–491, doi:10.1007/s11557-010-0717-y

Nakasone KK. 1997. Studies in *Phlebia*. Six species with teeth. Sydowia 49:49–79.

———. 2002. *Mycoaciella*, a synonym of *Phlebia*. Mycotaxon 81:477–490.

———, Burdsall HH. 1984. *Merulius*, a synonym of *Phlebia*. Mycotaxon 21:241–246.

Pond SL, Frost SD, Muse SV. HyPhy: hypothesis testing using phylogenies. Bioinformatics 21:676–679, doi:10.1093/bioinformatics/bti079

Rehner SA, Buckley EP. 2005. Cryptic diversification in *Beauveria bassiana* inferred from nuclear its and ef1-alpha phylogenies. Mycologia 97:84–98, doi:10.3852/mycologia.97.1.84

Ronquist F, Teslenko M, van der Mark P, Ayres DL, Darling A, Höhna S, Larget B, Liu L, Suchard MA, Huelsenbeck JP. 2012. MrBayes 3.2: efficient Bayesian phylogenetic inference and model choice across a large model space. Syst Biol 61:539–42, doi:10.1093/sysbio/sys029

Rokas A, Carroll SB. 2005. More genes or more taxa? The relative contribution of gene number and taxon number to phylogenetic accuracy. Mol Biol Evol 22: 1337–1344, doi:10.1093/molbev/msi121

Ryvarden L. 1991. Genera of polypores: nomenclature and taxonomy. Synopsis Fungorum 5. Oslo: Fungiflora.

Sanderson MJ. 2003. r8s: inferring absolute rates of molecular evolution and divergence times in the absence of a molecular clock. Bioinformatics 19:301–302, doi:10.1093/bioinformatics/19.2.301

Schmitt I, Crespo A, Divakar PK, Fankhauser JD, Herman-Sackett E, Kalb K, Nelsen MP, Nelson NA, Rivas-Plata E, Shimp AD, Widhelm T, Lumbsch HT. 2009. New primers for promising single-copy genes in fungal phylogenetics and systematics. Persoonia 23:35–40, doi:10.3767/003158509X470602

Simmons MP, Carr TG, O'Neill K. 2004. Relative character-state space, amount of potential phylogenetic information, and heterogeneity of nucleotide and amino acid characters. Mol Phylogenet Evol 32:913–26, doi:10.1016/j.ympev.2004.04.011

Sjökvist E, Larsson E, Eberhardt U, Ryvarden L, Larsson KH. 2012. Stipitate steriod basidiocarps have evolved multiple times. Mycologia 104:1046–1055, doi:10.3852/11-174

Sotome K, Hattori T, Ota Y, To-anun C, Salleh B, Kakishima M. 2008. Phylogenetic relationships of Polyporus and morphologically allied genera. Mycologia 100:603–15, doi:10.3852/07-191R

Stamatakis A. 2006. RAxML-VI-HPC: Maximum likelihood-based phylogenetic analyses with thousands of taxa and mixed models. Bioinformatics 22:2688–2690, doi:10.1093/bioinformatics/btl446

———, Hoover P, Rougemont J. 2008. A rapid bootstrap algorithm for the RAxML Web servers. Syst Biol 57: 758–771, doi:10.1080/10635150802429642

Talavera G, Castresana J. 2007. Improvement of phylogenies after removing divergent and ambiguously aligned blocks from protein sequence alignments. Syst Biol 56:564–577, doi:10.1080/10635150701472164

Townsend JP. 2007. Profiling phylogenetic informativeness. Syst Biol. 56:222–231, doi:10.1080/10635150701311362

———, Su Z, Tekle YI. 2012. Phylogenetic signal and noise: predicting the power of a dataset to resolve phylogeny. Syst Biol 61:835–849, doi:10.1093/sysbio/sys036

Walker DM, Castlebury LA, Rossman AY, White JF Jr. 2012. New molecular markers for fungal phylogenetics: two genes for species-level systematics in the Sordariomycetes (Ascomycota). Mol Phylogenet Evol 64:500–512, doi:10.1016/j.ympev.2012.05.005

Wapinski I, Pfeffer A, Friedman N, Regev A. 2007. Natural history and evolutionary principles of gene duplication in fungi. Nature 449:54–61, doi:10.1038/nature06107

Zhou LW, Dai YC. 2012. Wood-inhabiting fungi in southern China 5. New species of *Theleporus* and *Grammothele* (Polyporales, Basidiomycota). Mycologia 104:915–924, doi:10.3852/11-302

Supplementary files legends

SUPPLEMENTARY FIGURE 1. Correlation between genome size and gene numbers for 10 Polyporales genomes. (Bjead = *Bjekandera adusta;* Dicsq = *Dichomitus squalens;* Fompi = *Fomitopsis pinicola;* Gansp = *Ganoderma sp.;* Gersu = *Gelatoporia subversmispora;* Phchr = *Phanerochaete chrysosporium;* Phlbr = *Phlebia brevispora;* Rhopl = *Rhodonia placenta;* Trave = *Trametes versicolor;* Wolco = *Wolfiporia cocos*).

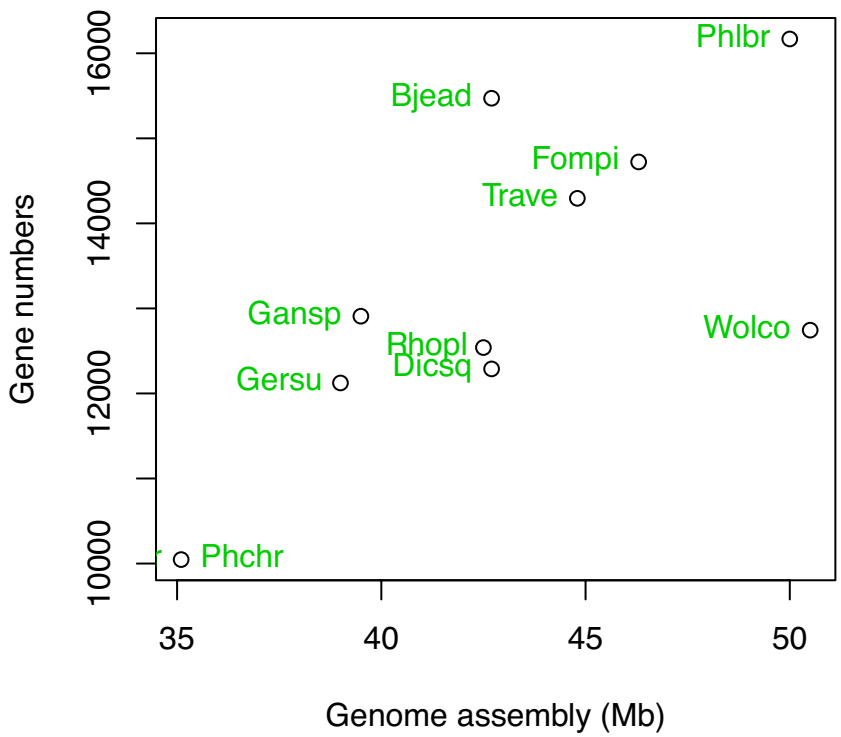
Phlbr
Bjead
Fompi
Trave
Gansp
Wolco
Rhopl
Dicsq
Gersu
Phchr
16000
14000
12000
10000
35
40
45
50
Gene numbers
Genome assembly (Mb)

Supplementary Table I. GenBank sequences used for the multilocus phylogenetic analyses

Taxon	**nLSU**	**ITS (5.8S)**	**nSSU**	**RPB1**	**RPB2**	**TEF1**
Abortiporus biennis (Bull.) Singer			EU232235			
Abundisporus sclerosetosus Decock & Laurence	FJ393868	FJ411101				
Abundisporus violaceus (Wakef.) Ryvarden	FJ393867	FJ411100				
Amauroderma rugosum (Blume & T. Nees) Torrend	AB368061	AB509712			AB368119	
Amylocystis lapponica (Romell) Bondartsev & Singer ex Singer	AF518598		AF518570			
Antrodia albida (Fr.) Donk, Persoonia	EU232272	EU232189	EU232240		DQ491387	
Antrodia albobrunnea (Romell) Ryvarden	EU232299	EU232215	EU232257			
Antrodia alpina (Litsch.) Gilb. & Ryvarden	EU232282	EU232207	EU232240			
Antrodia carbonica (Overh.) Ryvarden & Gilb.	EU232285	EU232211	EU232243		AY218470	
Antrodia heteromorpha (Fr.) Donk	AY515350	DQ491415			DQ491388	
Antrodia juniperina (Murrill) Niemelä & Ryvarden	EU232295	EU232212	EU232253		DQ491389	
Antrodia malicola (Berk. & M.A. Curtis) Donk	EU232297	EU232214	EU232255			
Antrodia odora (Peck ex Sacc.) Gilb. & Ryvarden	EU232286	EU232194	EU232244			
Antrodia oleracea (R.W. Davidson & Lombard) Ryvarden	EU232291	EU232198	EU232244			
Antrodia radiculosa (Peck) Gilb. & Ryvarden	EU232292	EU232201	EU232250			
Antrodia serialis (Fr.) Donk			EU232251			
Antrodia sinuosa (Fr.) P. Karst.	EU232288	EU232196	EU232246			
Antrodia sordida Ryvarden & Gilb.	EU232289	EU232193	EU232247			
Antrodia taxa T.T. Chang & W.N. Chou	EU232276	EU232192	EU232234			
Antrodia vaillantii (DC.) Ryvarden	EU232271	EU232188	EU232229			
Antrodia variiformis (Peck) Donk	AY515344	DQ491418			DQ491391	

Taxon	**nLSU**	**ITS (5.8S)**	**nSSU**	**RPB1**	**RPB2**	**TEF1**
Antrodia xantha (Fr.) Ryvarden	EU232284	DQ491424	EU232242		DQ491391	
Antrodiella americana Ryvarden & Gilb.	EU232270	EU232186	AY336781			
Antrodiella formosana T.T. Chang & W.N. Chou	EU232268	EU232184	EU232226			
Antrodiella liebmannii (Fr.) Ryvarden	EU232262	EU232178	EU232220			
Antrodiella pallasii Renvall, Johann. & Stenlid	EU232267	EU232183	EU232225			
Atraporiella neotropica Ryvarden	HQ659221	HQ659221				
Aurantiopileus mayanensis Ginns, D.L. Lindner & T.J. Baroni	HM772139	HM772140				
Auriporia aurea (Peck) Ryvarden	AF287846		AF334903		AY218471	
Bjerkandera adusta (Willd.) P. Karst.	AF287848	AY787666	DQ060085	genomic	genomic	genomic
Buglossoporus pulvinus (Pers.) Donk					DQ491392	
Bulbillomyces farinosus (Bres.) Jülich	DQ681201	DQ681201				
Byssomerulius corium (Pers.) Parmasto	AY586640					
Candelabrochaete africana Boidin	AF518604		AF518573			
Candelabrochaete septocystidia (Burt) Burds.	EU118609	EU118609				
Ceraceomyces eludens K.H. Larss.	AF090880					
Ceraceomyces microsporus K.H. Larss.	AF090873					
Ceraceomyces serpens (Tode) Ginns	AF090882					
Ceraceomyces sulphurinus (P. Karst.) J. Erikss. & Ryvarden	GU187610					
Ceraceomyces violascens (Fr.) Jülich	EU118612					
Ceriporia lacerata N. Maek., Suhara & R. Kondo	JN641759	JN641761	JN618335			
Ceriporia purpurea (Fr.) Donk	AF287852		AF026594		AY218476	
Ceriporia reticulata (Hoffm.) Domanski			AB084587			
Ceriporia tarda (Berk.) Ginns	GQ470632					

Taxon	**nLSU**	**ITS (5.8S)**	**nSSU**	**RPB1**	**RPB2**	**TEF1**
Ceriporia viridans (Berk. & Broome) Donk	AF393049		AF334905			
Ceriporiopsis aneirina (Sommerf.) Domanski	EU368503	EU340895				
Ceriporiopsis balaenae Niemelä	FJ496718	FJ496668				
Ceriporiopsis consobrina (Bres.) Ryvarden	FJ496716	FJ496667				
Ceriporiopsis gilvescens (Bres.) Domanski	FJ496720	FJ496684				
Ceriporiopsis guidella Bernicchia & Ryvarden	FJ496722	FJ496687				
Ceriporiopsis jelicii (Tortic & A. David) Ryvarden & Gilb.	FJ496727	FJ496690				
Ceriporiopsis resinascens (Romell) Domanski	FJ496703	FJ496679				
Ceriporiopsis rivulosa (Berk. & M.A. Curtis) Gilb. & Ryvarden	FJ496710	FJ496693				
Ceriporiopsis subrufa (Ellis & Dearn.) Ginns	FJ496724	FJ496662				
Cerrena aurantiopora J.S. Lee & Y.W. Lim	FJ821521	FJ821532			FJ821546	
Cerrena consors (Berk.) K.S. Ko & H.S. Jung	FJ821517	FJ821528			FJ821543	
Cinereomyces lindbladii (Berk.) Jülich	AY333814	HQ659223	AY336768			
Climacodon septentrionalis (Fr.) P. Karst.	AY684165	AY854082		AY864872	AY780941	AY885151
Coriolopsis aspera (Jungh.) Teng	AY351956					
Coriolopsis cf. *byrsina* (Mont.) Ryvarden	JN164788	JN165001		JN164838	JN164871	JN164879
Coriolopsis cf. *caperata* (Berk.) Murrill	JN164789	JN164999		JN164837	JN164870	JN164880
Coriolopsis gallica (Fr.) Ryvarden	JN164814	JN165013		JN164821	JN164869	
Coriolopsis sanguinaria (Klotzsch) Teng	AY351950					
*Coriolopsis trogii (*Berk.) Domanski	JN164808	JN164993		JN164820	JN164867	JN164898
Cryptoporus volvatus (Peck) Shear	AF393050		AF334907		AY218479	
Dacryobolus sudans (Alb. & Schwein.) Fr.	AY293176		AY293127			
Daedalea dickinsii Yasuda	EU024963	FJ810167				

Taxon	**nLSU**	**ITS (5.8S)**	**nSSU**	**RPB1**	**RPB2**	**TEF1**
Daedalea quercina (L.) Pers.			AF026600			
Daedaleopsis confragosa (Bolton) J. Schröt.	AB368062	GU731549	AF334908		AB368120	
Datronia mollis (Sommerf.) Donk	JN164791	JN165002	AF334909	JN164818	JN164872	JN164901
Datronia scutellata (Schwein.) Gilb. & Ryvarden	JN164792	JN165004		JN164817	JN164873	JN164902
Dentocorticium sulphurellum (Peck) M.J. Larsen & Gilb.	JN164815	JN165015		JN164841	JN164875	JN164903
Dichomitus campestris (Quél.) Domanski & Orlicz	AJ487512					
Dichomitus gunnii D.A. Reid	AJ487513					
Dichomitus squalens (P. Karst.) D.A. Reid	AJ487514	AM988624		genomic	genomic	genomic
Diplomitoporus crustulinus (Bres.) Domanski	AY333815	AF343320	AY336769			
Diplomitoporus flavescens (Bres.) Domanski	GU566006					
Diplomitoporus overholtsii (Pilát) Gilb. & Ryvarden	AY333813		AY336767			
Donkioporia expansa (Desm.) Kotl. & Pouzar	HM536052		HM536053		HM536102	HM536103
Earliella scabrosa (Pers.) Gilb. & Ryvarden	JN164793	JN165009	AY336766	JN164819	JN164866	JN164894
Echinochaete brachypora (Mont.) Ryvarden	AB462309	AB462321				
Echinochaete maximipora Sotome & T. Hatt.	AB462302	AB462314				
Echinochaete ruficeps (Berk. & Broome) Ryvarden	AB368066				AB368124	
Echinochaete russiceps (Berk. & Broome) D.A. Reid	AB462306	AB462318				
Epithele macarangae Boidin & Lanq.	DQ679923		DQ440638			
Epithele typhae (Pers.) Pat.	DQ457665	DQ486701				
Fomes fomentarius (L.) Fr.			AF026574			
Fomitella rhodophaea (Lév.) T. Hatt.	EU232300	EU232216	EU232258			
Fomitopsis africana Mossebo & Ryvarden					DQ491395	
Fomitopsis cajanderi (P. Karst.) Kotl. & Pouzar					DQ491372	

Taxon	**nLSU**	**ITS (5.8S)**	**nSSU**	**RPB1**	**RPB2**	**TEF1**
Fomitopsis cupreorosea (Berk.) J. Carranza & Gilb.	AY515325	DQ491400			DQ491373	
Fomitopsis dochmia (Berk. & Broome) Ryvarden	AY515326	DQ491401			DQ491374	
Fomitopsis feei (Fr.) Kreisel	AY515327	DQ491402			DQ491375	
Fomitopsis lilacinogilva (Berk.) J.E. Wright & J.R. Deschamps	AY515329	DQ491403			DQ491376	
Fomitopsis meliae (Underw.) Gilb.					DQ491394	
Fomitopsis officinalis (Batsch) Bondartsev & Singer	EU854447	EU854441				
Fomitopsis ostreiformis (Berk.) T. Hatt.	FJ372706	FJ372684				
Fomitopsis palustris (Berk. & M.A. Curtis) Gilb. & Ryvarden	AY515333	DQ491404			DQ491377	
Fomitopsis pinicola (Sw.) P. Karst.	AY684164	AY854083	AY705967	genomic	genomic	genomic
Fomitopsis rosea (Alb. & Schwein.) P. Karst.	AY333808	DQ491410	AY336764		DQ491383	
Fomitopsis spraguei (Berk. & M.A. Curtis) Gilb. & Ryvarden	AY515335	DQ491406			DQ491379	
Ganoderma australe (Fr.) Pat.	AY333807		AY336763			
Ganoderma lucidum (Curtis) P. Karst.	AB368068	EU021460	HQ697340		AB368126	
Ganoderma sp.				genomic	genomic	genomic
Ganoderma tsugae Murrill	AY684163	DQ206985	AY705969		DQ408116	DQ059048
Gelatoporia pannocincta (Romell) Niemelä	AF141612	AY219361				
Gelatoporia subvermispora (Pilát) Niemelä	FJ496707			genomic	genomic	genomic
Gloeoporus dichrous (Fr.) Bres.	DQ679919	EU546097				
Grammothele fuligo (Berk. & Broome) Ryvarden	AJ406506	GQ355956				
Grifola frondosa (Dicks.) Gray	AY629318	AY854084		AY864876		AY885153
Grifola sordulenta (Mont.) Singer	AY645050	AY854085		AY864877	AY786058	AY885154

Taxon	**nLSU**	**ITS (5.8S)**	**nSSU**	**RPB1**	**RPB2**	**TEF1**
Hapalopilus rutilans (Pers.) Murrill	AY293184		AY293133			
Heterobasidion annosum (Fr.) Bref.	AF287866	JF440572	AF026576	genomic	genomic	genomic
Hexagonia apiaria (Pers.) Fr.	AY351945					
Hexagonia hirta (P. Beauv.) Fr.	AY351944		AY336759			
Hexagonia hydnoides (Sw.) M. Fidalgo	AY351942					
Hexagonia pobeguinii Har.	AY333801					
Hexagonia tenuis (Hook.) Fr.	AY351935					
Hyphoderma cremeoalbum (Höhn. & Litsch.) Jülich	DQ677492	DQ677492				
Hyphoderma definitum (H.S. Jacks.) Donk	DQ677493	DQ677493				
Hyphoderma heterocystidiatum (Burt) Donk	DQ677495	DQ677495				
Hyphoderma incrustatum K.H. Larss.	AY586668					
Hyphoderma litschaueri (Burt) J. Erikss. & Å. Strid	DQ677496	DQ677496				
Hyphoderma medioburiense (Burt) Donk	DQ677497	DQ677497				
Hyphoderma mutatum (Peck) Donk	DQ677498	DQ677498				
Hyphoderma nemorale K.H. Larss.	AY586669					
Hyphoderma obtusum J. Erikss.	AY586670					
Hyphoderma occidentale (D.P. Rogers) Boidin & Gilles	DQ677499	DQ677499				
Hyphoderma roseocremeum (Bres.) Donk	AY586672					
Hyphoderma setigerum (Fr.) Donk	AY586673	GQ409531				
Hyphodermella corrugata (Fr.) J. Erikss. & Ryvarden	GQ470635	FN600372				
Hypochnicium cremicolor (Bres.) H. Nilsson & Hallenb.	DQ677506	DQ677506				
Hypochnicium eichleri (Bres. ex Sacc. & P. Syd.) J. Erikss. & Ryvarden	FJ471542					

Taxon	**nLSU**	**ITS (5.8S)**	**nSSU**	**RPB1**	**RPB2**	**TEF1**
Hypochnicium erikssonii Hallenb. & Hjortstam	DQ677508	DQ677508				
Hypochnicium geogenium (Bres.) J. Erikss.	JN939576	AF429426	JN940193			
Hypochnicium karstenii (Bres.) Hallenb.	DQ677510	DQ677510				
Hypochnicium michelii Tellería, M. Dueñas, Melo & M.P. Martín	JN939579	FN552535				
Hypochnicium polonense (Bres.) Å. Strid	EU118635	EU118635				
Hypochnicium wakefieldiae (Bres.) J. Erikss.	JN939578	FN552533				
Ischnoderma resinosum (Schrad.) P. Karst.	AJ487927	GU731564				
Junghuhnia nitida (Pers.) Ryvarden	EU118638	EU118638				
Laetiporus cincinnatus (Morgan) Burds.	EU402521	EU402557				AB472661
Laetiporus conifericola Burds. & Banik	EU402524	EU402577				AB472664
Laetiporus gilbertsonii Burds.	EU402527	EU402549				AB472666
Laetiporus huroniensis Burds. & Banik	EU402540	EU402571				AB472670
Laetiporus montanus Cerný ex Tomsovský & Jankovský	EU884419	EU840558				
Laetiporus persicinus (Berk. & M.A. Curtis) Gilb.	EU402513	EU402579				
Laetiporus sulphureus (Bull.) Murrill	AY684162	DQ221108	AY705966		DQ408118	
Lentinus bertieri (Fr.) Fr.	AY615986	GU207302				
Lentinus crinitus (L.) Fr.	AY615979	GU207291				
Lentinus squarrosulus Mont.	AB368071	GU001951			AB368129	
Lentinus suavissimus Fr.	AY615970					
Lentinus swartzii Berk.	AY615983	GU207276				
Lentinus tigrinus (Bull.) Fr.	AB368072	AF516520	AF026571		AB368130	
Leptoporus mollis (Pers.) Quél.	EU402510	EU402584				
Lignosus hainanensis B.K. Cui	GU580885	GU580883				

Taxon	**nLSU**	**ITS (5.8S)**	**nSSU**	**RPB1**	**RPB2**	**TEF1**
Lignosus rhinocerus (Cooke) Ryvarden	AB368074	FJ380871			AB368132	
Lopharia cinerascens (Schwein.) G. Cunn.	JN164813	JN165019			JN164874	JN164900
Megasporoporia cavernulosa (Berk.) Ryvarden	AY333800		AY336757			
Megasporoporia setulosa (Henn.) Rajchenb.	GU566007					
Melanoporia nigra (Berk.) Murrill					DQ491393	
Meripilus giganteus (Pers.) P. Karst.	AF287874		AF026568		AY218496	
Microporus affinis (Blume & T. Nees) Kuntze	AY351931					
Microporus vernicipes (Berk.) Imazeki	AY351929	AB531465				
Microporus xanthopus (Fr.) Kuntze	AB368075	AJ698132	AY336756		AB368133	
Mycoacia aurea (Fr.) J. Erikss. & Ryvarden	AY586691					
Mycoaciella bispora (Stalpers) J. Erikss. & Ryvarden	AY586692					
Mycobonia flava (Berk.) Pat.	AJ487933	AY513570				
Neolentiporus maculatissimus (Lloyd) Rajchenb.	AF518632				AY218497	
Obba valdiviana (Rajchenb.) Miettinen & Rajchenb.	HQ659235	HQ659235				
Oligoporus lacteus (Fr.) Gilb. & Ryvarden	AY293205		AY293152		AY218510	
Oligoporus rennyi (Berk. & Broome) Donk			AF334922			
Panus ciliatus (Lév.) T.W. May & A.E. Wood	AY616006					
Panus conchatus (Bull.) Fr.	AY616003					
Panus fasciatus (Berk.) Singer	EU908180					
Panus fulvus (Berk.) Pegler & R.W. Rayner	AY615996					
Panus lecomtei (Fr.) Corner	AY615995					
Panus rudis Fr.	AF287878		AF026569			
Panus similis (Berk. & Broome) T.W. May & A.E. Wood	AY616000					

Taxon	nLSU	ITS (5.8S)	nSSU	RPB1	RPB2	TEF1
Panus strigellus (Berk.) Overh.	AY616002					
Panus velutinus (Fr.) Fr.	GQ487335					
Parmastomyces transmutans (Overh.) Ryvarden & Gilb.	AF518635		AY293143			
Perenniporia corticola (Corner) Decock	HQ654108	HQ654094				
Perenniporia cystidiata Y.C. Dai, W.N. Chou & Sheng H. Wu	HQ654113					
Perenniporia detrita (Berk.) Ryvarden	FJ393866	FJ411099				
Perenniporia fraxinea (Bull.) Ryvarden	HQ654110	HQ654095				
Perenniporia japonica (Yasuda) T. Hatt. & Ryvarden	HQ654111	HQ654097				
Perenniporia medullapanis (Jacq.) Donk			AF334924			
Perenniporia minor Y.C. Dai & Xiong	HQ654115	HQ848475				
Perenniporia ochroleuca (Berk.) Ryvarden	FJ393864	FJ411097				
Perenniporia ohiensis (Berk.) Ryvarden	FJ393863	FJ411096				
Perenniporia rhizomorpha B.K. Cui, Y.C. Dai & Decock	HQ654117	HQ654107				
Perenniporia subacida (Peck) Donk	FJ393880	FJ411103				
Perenniporiella chaquenia Robledo & Decock	FJ393856	FJ411084				HM467610
Perenniporiella micropora (Ryvarden) Decock & Ryvarden	FJ393858	FJ411086				HM467608
Perenniporiella neofulva (Lloyd) Decock & Ryvarden	FJ393852	FJ411080				HM467599
Perenniporiella pendula Decock & Ryvarden	J393854	FJ411082				HM467600
Perenniporiella tepeitensis (Murrill) Decock & Valenzuela	HM467594	HM467589				HM467603
Phaeolus schweinitzii (Fr.) Pat.	AY629319		AY705961		DQ408119	DQ028602
Phanerochaete aculeata Hallenb.	GQ470636					
Phanerochaete angustocystidiata Sheng H. Wu	GQ470637					
Phanerochaete argillacea Sheng H. Wu	GQ470656					

Taxon	**nLSU**	**ITS (5.8S)**	**nSSU**	**RPB1**	**RPB2**	**TEF1**
Phanerochaete brunnea Sheng H. Wu	GQ470657					
Phanerochaete brunneocystidiata Sheng H. Wu	GQ470639					
Phanerochaete calotricha (P. Karst.) J. Erikss. & Ryvarden	FJ471565	EU047803				
Phanerochaete canolutea Sheng H. Wu	GQ470641					
Phanerochaete carnosa (Burt) Parmasto	GQ470642					
Phanerochaete chrysosporium Burds.	AF287883	AY854086		genomic	genomic	genomic
Phanerochaete crassa (Lév.) Burds.	GQ470634					
Phanerochaete deflectens (P. Karst.) Hjortstam	GQ470644					
Phanerochaete flavidoalba (Cooke) S.S. Rattan	GQ470667					
Phanerochaete ginnsii Sheng H. Wu	GQ470645					
Phanerochaete intertexta Sheng H. Wu	GQ470646					
Phanerochaete lamprocystidiata Sheng H. Wu	GQ470648					
Phanerochaete laxa Sheng H. Wu	GQ470649					
Phanerochaete leptoderma Sheng H. Wu	GQ470650					
Phanerochaete lutea (Sheng H. Wu) Hjortstam	GQ470651					
Phanerochaete odontoidea Sheng H. Wu	GQ470652					
Phanerochaete parmastoi Sheng H. Wu	GQ470654					
Phanerochaete sanguinea (Fr.) Pouzar	GQ470655					
Phanerochaete sordida (P. Karst.) J. Erikss. & Ryvarden	GQ470658					
Phanerochaete stereoides Sheng H. Wu	GQ470661					
Phanerochaete subglobosa Sheng H. Wu	GQ470662					
Phanerochaete subodontoidea Sheng H. Wu	GQ470664					
Phanerochaete taiwaniana Sheng H. Wu	GQ470666					

Taxon	**nLSU**	**ITS (5.8S)**	**nSSU**	**RPB1**	**RPB2**	**TEF1**
Phanerochaete tropica (Sheng H. Wu) Hjortstam	GQ470672					
Phanerochaete tuberculata (P. Karst.) Parmasto	GQ470669					
Phanerochaete velutina (DC.) P. Karst.	DQ679917					
Phlebia acerina Peck	AF141615	AF141615				
Phlebia albomellea (Bondartsev) Nakasone	AY293198		AY293144			
Phlebia bresadolae Parmasto	AF141617	AF141617				
Phlebia brevispora Nakasone				genomic	genomic	genomic
Phlebia centrifuga P. Karst.	AF141618	AF141618				
Phlebia chrysocreas (Berk. & M.A. Curtis) Burds.	AY586695	HQ153411	AY293145			
Phlebia deflectens (P. Karst.) Ryvarden	AF141619	AF141619				
Phlebia lilascens (Bourdot) J. Erikss. & Hjortstam	AF141622	AF141622				
Phlebia livida (Pers.) Bres.	AF141624	AF141624				
Phlebia nitidula (P. Karst.) Ryvarden	EU118655	EU118655				
Phlebia nothofagi (G. Cunn.) Nakasone	GU226430					
Phlebia queletii (Bourdot & Galzin) M.P. Christ.	AF141626	AF141626				
Phlebia radiata Fr.	AF287885	AY854087		AY864881	AY218502	AY885156
Phlebia rufa (Pers.) M.P. Christ.	AF141628	AF141628				
Phlebia setulosa (Berk. & M.A. Curtis) Nakasone	GU461311	GU46131				
Phlebia subserialis (Bourdot & Galzin) Donk	AF141631	AF141631				
Phlebia uda (Fr.) Nakasone	AF141614	AF141614				
Phlebiopsis flavidoalba (Cooke) Hjortstam	EU118662	EU118662				
Phlebiopsis himalayensis Dhingra	GQ470673					
Phlebiopsis roumeguerii (Bres.) Jülich & Stalpers	GQ470675					

Taxon	**nLSU**	**ITS (5.8S)**	**nSSU**	**RPB1**	**RPB2**	**TEF1**
Physisporinus vitreus (Pers.) P. Karst.	FJ496726	JN182920				
Piptoporus portentosus (Berk.) G. Cunn.	AY515353					
Podoscypha multizonata (Berk. & Broome) Pat.	EU118663	EU118663				
Podoscypha parvula (Lloyd) D.A. Reid	AF261534					
Podoscypha petalodes (Berk.) Pat.	AF518639		AY293149			
Polyporus alveolaris (DC.) Bondartsev & Singer	AB368079	AB587624			AB368136	
Polyporus arcularius (Batsch) Fr.	AB368081	AF516523	AF334928		AB368138	
Polyporus badius (Pers.) Schwein.	AB368083	AB587625			AB368140	
Polyporus brumalis (Pers.) Fr.	AB368084	FJ596883			AB368141	
Polyporus ciliatus Fr.	AJ487943	AB070882				
Polyporus craterellus Berk. & M.A. Curtis	AJ487944					
Polyporus dictyopus Mont.	AB368086				AB368143	
Polyporus grammocephalus Berk.	AB368090	AB587627			AB368148	
Polyporus guianensis Mont.	AJ487947	AF516564				
Polyporus leprieurii Mont.	AJ487949	AF516567			AB368150	
Polyporus melanopus (Pers.) Fr.	AF261545	AF518759	AF334929		AY218507	
Polyporus meridionalis (A. David) H. Jahn	AJ487952					
Polyporus pseudobetulinus (Murashk. ex Pilát) Thorn, Kotir. & Niemelä	AB587639	AB587644				
Polyporus radicatus Schwein.	AJ487956					
Polyporus rhizophilus Pat.	AJ487957					
Polyporus squamosus (Huds.) Fr.	AY629320	DQ267123	AY705963	DQ831023	DQ408120	DQ028601
Polyporus subvarius C.J. Yu & Y.C. Dai	AB587638	AF516585				

Taxon	nLSU	ITS (5.8S)	nSSU	RPB1	RPB2	TEF1
Polyporus tenuiculus (P. Beauv.) Fr.	AB368099				AB368156	
Polyporus tricholoma Mont.	AB368100	AF516555			AB368157	
Polyporus tubaeformis (P. Karst.) Ryvarden & Gilb.	AB368101	AB587634			AB368158	
Polyporus tuberaster (Jacq. ex Pers.) Fr.	AF261544	AY218420	AF334930		AB368162	
Polyporus udus Jungh.	AB368108	AF518756			AB368165	
Polyporus umbellatus (Pers.) Fr. :354	AB368109	EU442276			AB368166	
Polyporus varius (Pers.) Fr.	AB368112				AB368169	
Polyporus virgatus Berk. & M.A. Curtis	AJ488122	AF516581				
Porostereum spadiceum (Pers.) Hjortstam & Ryvarden	DQ679918					
Postia caesia (Schrad.) P. Karst.	AB569119					
Postia japonica Y.C. Dai & T. Hatt.	AB569122					
Postia leucomallella (Murrill) Jülich	AF393072		AF334932			
Postia stellifera T. Hatt. & Sotome	AB569123					
Pseudofavolus cucullatus (Mont.) Pat.	AB368114	AF516601			AB368170	
Pseudolagarobasidium acaciicola Ginns	EU569321					
Pseudolagarobasidium calcareum (Cooke & Massee) Sheng H. Wu	EU569320					
Pseudolagarobasidium subvinosum (Berk. & Broome) Sheng H. Wu	EU569319					
Pulcherricium caeruleum (Lam.) Parmasto	GQ470677		AF334933			
Pyrofomes demidoffii (Lév.) Kotl. & Pouzar	FJ393873	FJ411105				
Radulodon americanus Ryvarden	EU569322					
Radulodon erikssonii Ryvarden	EU569325					
Rhizochaete americana (Nakasone, C.R. Bergman & Burds.) Gresl.,	AY219391	AY219391	AY219396			

Taxon	**nLSU**	**ITS (5.8S)**	**nSSU**	**RPB1**	**RPB2**	**TEF1**
Nakasone & Rajchenb.						
Rhizochaete brunnea Gresl., Nakasone & Rajchenb.	AY219389	AY219389	AY219395			
Rhizochaete filamentosa (Berk. & M.A. Curtis) Gresl., Nakasone & Rajchenb.	AY219393	AY219393	AY219398			
Rhizochaete fouquieriae (Nakasone & Gilb.) Gresl., Nakasone & Rajchenb.	AY219390	AY219390	AY219397			
Rhizochaete radicata (Henn.) Gresl., Nakasone & Rajchenb.	AY219392	AY219392	AY219399			
Rhodonia placenta (Fr.) Niemelä, K.H. Larss. & Schigel				genomic	genomic	genomic
Rigidoporus microporus (Sw.) Overeem	AY333795					
Rigidoporus vinctus (Berk.) Ryvarden	AY333794		AY336752			
Scopuloides hydnoides (Cooke & Massee) Hjortstam & Ryvarden	EU118665	EU118665				
Scopuloides rimosa (Cooke) Jülich	GQ470676					
Sebipora aquosa Miettinen	HQ659240	HQ659240				
Skeletocutis amorpha (Fr.) Kotl. & Pouzar	AY293214	FN907913				
Skeletocutis chrysella Niemelä	FN907916	FN907916				
Sparassis brevipes Krombh.	AY218403	AY218441	AY218381		AY218543	
Sparassis crispa (Wulfen) Fr.	AY629321	DQ250597	AY705962		DQ408122	DQ056289
Sparassis cystidiosa Desjardin & Zheng Wang	AY256890	AY256891			AY256892	
Sparassis radicata Weir	AY218410	AY218449			AY218546	
Sparassis spathulata (Schwein.) Fr.	AY218392	AY218429	AY218378		AY218536	
Sparsitubus nelumbiformis L.W. Hsu & J.D. Zhao	DQ887631					
Spongipellis delectans (Peck) Murrill	HQ729008	HQ728299				
Spongipellis litschaueri Lohwag	HQ729015	HQ728307				

Taxon	**nLSU**	**ITS (5.8S)**	**nSSU**	**RPB1**	**RPB2**	**TEF1**
Spongipellis pachyodon (Pers.) Kotl. & Pouzar	AY629322	DQ249277	DQ457638		DQ408123	DQ028599
Spongipellis spumeus (Sowerby) Pat.	HQ729021	HQ728287				
Spongipellis unicolor (Schwein.) Murrill	HQ729011	HQ728313				
Steccherinum fimbriatum (Pers.) J. Erikss.	EU118668	EU118668	AF518590			
Steccherinum robustius (J. Erikss. & S. Lundell) J. Erikss.	EU118671	EU118671				
Stereum hirsutum (Willd.) Pers.	AF393078	AY854063	AF026588	genomic	genomic	genomic
Taiwanofungus camphoratus (M. Zang & C.H. Su) Sheng H. Wu, Z.H. Yu, Y.C. Dai & C.H. Su	EU232281	EU232205	EU232239			
Taiwanofungus salmoneus (T.T. Chang & W.N. Chou) Sheng H. Wu, Z.H. Yu, Y.C. Dai & C.H. Su	EU232279	EU232203	EU232237			
Trametes aff maxima	JN164802	JN164933		JN164836	JN164863	JN164884
Trametes betulina (L.) Pilát	JN164794	JN164983		JN164822	JN164860	JN164895
Trametes cinnabarina (Jacq.) Fr.	AY684160	DQ411525		JN164843	DQ408121	DQ02860
Trametes conchifer (Schwein.) Pilát	JN164797	JN164924	JF972593	JN164823	JN164849	JN164887
Trametes cubensis (Mont.) Sacc.	JN164798	JN164923		JN164834	JN164865	JN164883
Trametes ectypa (Berk. & M.A. Curtis) Gilb. & Ryvarden	JN164803	JN164929		JN164824	JN164848	JN164888
Trametes elegans (Spreng.) Fr.	JN164799	JN164944		JN164833	JN164861	JN164899
Trametes gibbosa (Pers.) Fr.	JN164800	JN164943		JN164831	JN164859	JN164896
Trametes hirsuta (Wulfen) Lloyd	JN164801	JN164941	JF972590	JN164829	JN164854	JN164891
Trametes junipericola Manjón, G. Moreno & Ryvarden	AY855915	AY684171				
Trametes ljubarskii Pilát	AY855911	AY684174				
Trametes maxima (Mont.) A. David & Rajchenb.	JN164804	JN164957		JN164816	JN164864	JN164885
Trametes membranacea (Sw.) Kreisel	JN164805	JN164945		JN164832	JN164857	JN164893

Taxon	**nLSU**	**ITS (5.8S)**	**nSSU**	**RPB1**	**RPB2**	**TEF1**
Trametes ochracea (Pers.) Gilb. & Ryvarden	JN164812	JN164954		JN164826	JN164852	JN164904
Trametes pavonia (Berk.) Fr.	JN164806	JN164958		JN164835	JN164862	JN164886
Trametes pocas (Berk.) Ryvarden	AY351919					
Trametes polyzona (Pers.) Justo	JN164790	JN164978		JN164844& JN164846	JN164856	JN164881
Trametes pubescens (Schumach.) Pilát	JN164811	JN164963		JN164827	JN164851	JN164889
Trametes punicea Fr.	FJ372708	FJ372686				
Trametes sanguinea (L.) Lloyd	JN164795	JN164982		JN164842	JN164858	JN164897
Trametes suaveolens (L.) Fr.	JN164807	JN164966	AF026572	JN164828	JN164853	JN164890
Trametes versicolor (L.) Lloyd	JN164809	JN164919	AY705965	genomic	genomic	genomic
Trametes villosa (Sw.) Kreisel	JN164810	JN164969		JN164830	JN164855	JN164892
Trametopsis cervina (Schwein.) Tomsovský	JN164796	JN165020		JN164839	JN164877	JN164882
Tyromyces chioneus (Fr.) P. Karst.	AF393080	AY636061	AF334938			
Tyromyces fissilis (Berk. & M.A. Curtis) Donk	HQ729002	HQ728292				
Vanderbylia vicina (Lloyd) D.A. Reid	FJ393862	FJ411095				
Wolfiporia cocos (F.A. Wolf) Ryvarden & Gilb.	EU402519	AY72827		genomic	genomic	genomic
Wolfiporia dilatohypha Ryvarden & Gilb.	EU402517	EU402556				
Xanthoporus syringae (Parmasto) Audet	AY684166	AY789078	AY707091	AY788846	AY780935	DQ059049

Supplementary Table II. New sequences generated during this study

Taxon	**Voucher (Herbarium)**	**nLSU & 5.8S**	**RPB2**	**TEF1**
Abortiporus biennis (Bull.) Singer	EL 65/03 (GB)	JN649325	JX109864	JX109892
Antrodia serialis (Fr.) Donk	KHL 12010 (GB)	JX109844	JX109870	JX109898
Antrodiella semisupina (Berk. & M.A. Curtis) Ryvarden	KHL 11977 (GB)	JX109842	JX109868	JX109896
Ceriporia reticulata (Hoffm.) Domanski	KHL 11981 (GB)	JX109845	JX109871	JX109899
Cerrena unicolor (Bull.) Murrill	K.H. Larsson s.n.(GB)	JQ031127	JX109863	JX109891
Climacocystis borealis (Fr.) Kotl. & Pouzar	KHL 13318 (GB)	JQ031126	JX109880	JX109909
Daedalea quercina (L.) Pers.	Miettinen 12662(H)	JQ700296	JX109883	JX109912
Fomes fomentarius (L.) Fr.	ES2008-3 (GB)	JX109860	JX109888	
Gloeoporus taxicola (Pers.) Gilb. & Ryvarden	SK 0075 (GB)	JX109847	JX109873	JX109901
Hydnopolyporus fimbriatus (Fr.) D.A. Reid	Meijer3729 (O)	JN649346	JX109875	JX109904
Hypochnicium lyndoniae (D.A. Reid) Hjortstam	NL 041031 (GB)	JX124704	JX109876	JX109905
Hypochnicium subrigescens Boidin	KHL 11968 (GB)	JQ031128	JX109877	JX109906
Irpex lacteus (Fr.) Fr.	DO 421/951208 (O)	JX109852	JX109882	JX109911
Ischnoderma benzoinum (Wahlenb.) P. Karst.	KHL 12099 (GB)	JX109841	JX109867	JX109895
Mycoacia fuscoatra (Fr.) Donk	KHL 13275 (GB)	JN649352	JX109879	JX109908
Nigroporus vinosus (Berk.) Murrill	BHS2008-100 (GB)	JX109857	JX109885	JX109914
Oligoporus rennyi (Berk. & Broome) Donk	TN 7389 (H)	JX109849	JX109874	JX109903
Pachykytospora tuberculosa (Fr.) Kotl. & Pouzar	KA11 (GB)	JX124705	JX109878	JX109907
Parmastomyces mollissimus (Maire) Pouzar	TN 7672 (H)	JX109848		JX109902
Perenniporia medulla-panis (Jacq.) Donk	KHL 11943 (GB)	JX109840	JX109866	JX109894
Phlebia firma J. Erikss. & Hjortstam	K268 (GB)	EU118654	JX109890	

Taxon	**Voucher (Herbarium)**	**nLSU & 5.8S**	**RPB2**	**TEF1**
Phlebia subochracea (Bres.) J. Erikss. & Ryvarden	KGN 162-95 (GB)	EU118656		
Phlebia tremellosa (Schrad.) Nakasone & Burds.	ES2008-2 (GB)	JX109859	JX109887	JX109916
Phlebia unica (H.S. Jacks. & Dearden) Ginns	KHL 11786 (GB)	EU118657	JX109861	JX109889
Physisporinus sanguinolentus (Alb. & Schwein.) Pilát	KHL 11913 (GB)	JX109843	JX109869	JX109897
Piloporia sajanensis (Parmasto) Niemelä	HK 17250 (GB)	JX109853		
Piptoporus betulinus (Bull.) P. Karst.	Miettinen 12388 (H)	JX109856	JX109884	JX109913
Podoscypha venustula (Speg.) D.A. Reid	LR 40821 (O)	JX109851	JX109881	JX109910
Porogramme albocincta (Cooke & Massee) J. Lowe	TL 9894/03	JX109854		
Postia placenta (Fr.) M.J. Larsen & Lombard	TN 7609 (GB)	JX109846	JX109872	JX109900
Postia tephroleuca (Fr.) Jülich	TN 6900(H)	JX109850		
Skeletocutis nivea (Jungh.) Jean Keller	ES2008-1 (GB)	JX109858	JX109886	JX109915
Steccherinum ochraceum (Pers. ex J.F. Gmel.) Gray	KHL 11902 (GB)	JQ031130	JX109865	JX109893

Supplementary Table III. Number of BBH ortologies in the 10 Polyporales genomes plus 5 outgroups

	Bjead	Gersu	Dicsq	Fompi	Gansp	Phchr	Rhopl	Trave	Wolco	Phlbr	Fomme	Punst	Glotr	Hetan
(total)	15473	12125	12290	14724	12910	10048	12541	14296	12746	16170	11333	11538	11846	13378
Gersu	6201													
Dicsq	6624	6186												
Fompi	6761	6243	6652											
Gansp	6850	6277	***8137***	6815										
Phchr	6617	***5387***	5717	5806	5874									
Rhopl	6470	6058	6361	6988	6554	5592								
Trave	6867	6330	7520	6888	7701	5863	6538							
Wolco	6622	6180	6473	7118	6683	5703	7025	6659						
Phlbr	7481	6236	6627	6778	6891	6380	6501	6859	6658					
Fomme	5938	5382	5727	5812	5918	5167	5620	5822	5784	5906				
Punst	6279	5622	6003	6159	6196	5420	5901	6166	5986	6253	5634			
Glotr	6695	6041	6415	6671	6636	5781	6384	6605	6512	6700	5971	6372		
Hetan	6423	5778	6165	6328	6398	5516	6107	6323	6233	6389	5830	6029	6481	
Stehi	6569	5936	6345	6506	6570	5642	6185	6520	6332	6560	5892	6254	6687	6756

Supplementary Table IV. Average percent identity between orthologs in the 10 Polyporales genomes plus 5 outgroups

	Bjead	Gersu	Dicsq	Fompi	Gansp	Phchr	Rhopl	Trave	Wolco	Phlbr	Fomme	Punst	Glotr	Hetan
Gersu	61													
Dicsq	61	63												
Fompi	60	63	62											
Gansp	60	63	***76***	62										
Phchr	67	63	62	61	62									
Rhopl	61	65	63	67	63	63								
Trave	61	63	70	62	69	62	63							
Wolco	61	64	63	67	62	62	69	63						
Phlbr	64	62	61	60	61	65	62	61	62					
Fomme	56	57	57	56	57	58	57	57	57	57				
Punst	58	59	59	58	58	59	59	58	59	58	57			
Glotr	59	60	60	59	59	60	60	59	60	59	57	60		
Hetan	59	60	60	59	59	60	60	60	60	59	57	59	60	
Stehi	57	58	58	57	57	58	58	57	58	57	56	57	58	64

Supplementary Table V. Number of orthologs in syntenic regions in the 10 Polyporales genomes plus 5 outgroups

	Bjead	Gersu	Dicsq	Fompi	Gansp	Phchr	Rhopl	Trave	Wolco	Phlbr	Fomme	Punst	Glotr	Hetan
(total)	15473	12125	12290	14724	12910	10048	12541	14296	12746	16170	11333	11538	11846	13378
Gersu	3417													
Dicsq	3777	3993												
Fompi	3759	3894	4341											
Gansp	4017	4191	***7289***	4486										
Phchr	5212	***3229***	3193	3175	3397									
Rhopl	3980	4304	4372	5581	4466	3414								
Trave	3731	4038	6164	4225	6568	3293	4355							
Wolco	4153	4452	4673	5844	5083	3587	6302	4804						
Phlbr	5202	3582	3675	3881	3991	4454	3806	3849	4330					
Fomme	2042	2106	2102	2065	2450	1764	2199	2201	2487	2261				
Punst	2718	2680	2627	2652	2999	2166	2784	2817	3135	2700	2234			
Glotr	3528	3488	3468	3406	4012	3139	3923	3660	4007	3437	2753	3663		
Hetan	3296	3202	3307	3189	3610	2767	3442	3506	3875	3350	2622	3137	4331	
Stehi	2183	2300	2346	2319	2823	1772	2671	2344	2881	2208	1906	2448	3304	4152

Supplementary Table VI. Top 30 pfam domains in 10 Polyporales. (The last 3 numbers are average, maximum and minimum PFAM counts in other 28 Basidiomycota)

	Bjead	Gersu	Dicsq	Fompi	Gansp	Phchr	Rhopl	Trave	Wolco	Phlbr	Other Basidiomycota			
											AVG	MAX	MIN	
PF00067	176	192	158	147	182	113	178	176	166	180	93.6	212	4	## p450
PF00400	197	169	183	125	151	109	104	116	129	129	131.3	275	80	## WD40
PF00069	146	143	114	124	122	106	116	126	120	126	117.1	229	69	## Pkinase
PF00646	164	88	93	110	106	70	105	160	80	114	118.4	784	7	## F-box
PF00106	74	91	94	143	88	84	120	122	125	109	75.1	177	14	## adh_short
PF00271	86	89	89	84	75	59	82	77	88	114	84.9	158	56	## Helicase_C
PF00172	69	70	77	56	82	35	44	84	66	70	59.3	149	5	## Zn_clus
PF00096	63	53	50	63	55	35	94	60	53	68	53.5	115	15	## zf-C2H2
PF00076	66	57	57	62	56	50	57	58	59	65	59.0	79	35	## RRM_1
PF00248	62	58	57	50	48	53	55	65	53	66	36.6	72	9	## Aldo_ket_red
PF00107	41	52	59	58	44	52	57	72	57	63	35.1	77	11	## ADH_zinc_N
PF00097	65	51	49	61	53	28	47	49	54	58	44.4	102	16	## zf-C3HC4
PF01370	46	45	56	56	43	50	44	50	54	61	37.9	84	11	## Epimerase
PF00270	49	53	51	57	48	33	49	48	50	66	49.2	75	36	## DEAD
PF08240	39	53	55	46	41	47	45	70	52	55	33.5	71	12	## ADH_N
PF00026	53	41	44	40	49	52	45	51	39	55	25.1	68	2	## Asp
PF00005	46	48	38	45	39	50	41	45	37	52	39.2	68	23	## ABC_tran
PF02985	43	47	43	38	44	42	39	45	47	43	39.3	61	30	## HEAT
PF00004	46	40	43	46	38	39	40	44	43	49	37.3	51	27	## AAA
PF01753	80	33	31	53	35	23	18	81	20	48	41.6	225	1	## zf-MYND
PF04082	48	35	39	38	45	36	35	43	44	45	37.8	72	2	## Fungal_trans
PF08659	27	45	37	56	40	27	35	48	47	38	27.2	67	8	## KR
PF00083	39	37	40	40	37	39	35	45	44	43	38.4	80	10	## Sugar_tr
PF06985	0	8	112	0	90	0	0	159	8	0	5.6	63	0	## HET
PF00098	25	31	30	15	40	57	92	28	41	17	40.0	154	5	## zf-CCHC
PF07993	39	23	35	35	36	29	42	41	45	48	27.3	68	7	## NAD_binding_4
PF01494	31	31	36	45	48	31	32	38	43	37	25.8	72	3	## FAD_binding_3
PF00561	41	30	37	39	40	27	27	56	28	41	25.8	59	8	## Abhydrolase_1
PF00153	37	34	34	36	37	34	35	35	37	38	34.0	39	29	## Mito_carr
PF01266	44	28	33	40	41	35	28	31	37	34	29.9	56	12	## DAO

Supplementary Table VII. Domains occurring at least in one Polyporales genome more often that in all Basidiomycota. (The last 3 numbers are average, maximum and minimum PFAM counts in other 28 Basidiomycota)

	Bjead	Gersu	Dicsq	Fompi	Gansp	Phchr	Rhopl	Trave	Wolco	Phlbr	Other Basidiomycota AVG	MAX	MIN		
PF00702	27	29	34	32	39	25	28	25	30	34	25.2	34	13	##	Hydrolase
PF00173	26	25	23	25	22	23	25	24	29	32	21.1	28	9	##	Cyt-b5
PF03171	20	24	34	30	31	16	25	22	25	31	14.2	25	1	##	2OG-FeII_Oxy
PF01423	14	13	16	19	16	13	15	16	16	15	14.7	18	11	##	LSM
PF00036	19	15	15	14	17	18	14	16	12	19	14.2	18	10	##	efhand
PF06985	0	8	112	0	90	0	0	159	8	0	5.6	63	0	##	HET
PF00450	30	14	18	9	18	21	15	24	11	24	10.8	28	2	##	Peptidase_S10
PF07859	13	23	19	8	9	8	19	30	11	16	10.0	19	2	##	Abhydrolase_3
PF09286	4	19	25	29	22	9	23	28	17	28	7.4	21	0	##	Pro-kuma_activ
PF00010	12	9	10	19	11	11	11	11	11	11	9.8	15	3	##	HLH
PF01764	9	6	15	8	19	8	6	11	10	14	9.2	18	0	##	Lipase_3
PF00487	14	10	9	10	11	6	11	16	10	18	8.3	15	3	##	FA_desaturase
PF04140	19	24	13	12	18	9	16	14	11	23	6.5	19	1	##	ICMT
PF01794	12	8	10	12	9	10	10	14	8	8	8.6	12	1	##	Ferric_reduct
PF08022	12	8	10	12	9	11	9	13	8	8	8.3	12	2	##	FAD_binding_8
PF00891	13	13	5	9	6	10	9	6	10	26	7.6	22	0	##	Methyltransf_2
PF00291	8	8	9	11	9	10	9	11	10	8	7.8	10	5	##	PALP
PF00046	11	7	9	11	14	7	8	9	6	11	7.7	12	1	##	Homeobox
PF00013	8	8	13	8	8	8	9	8	7	8	7.9	9	6	##	KH_1
PF02133	9	5	12	16	9	6	15	11	13	10	6.1	15	0	##	Transp_cyt_pur
PF00533	7	9	7	10	9	6	8	8	8	8	6.9	9	4	##	BRCT
PF01040	6	8	8	5	6	7	8	8	11	20	5.8	17	1	##	UbiA
PF01553	8	6	7	8	7	4	8	7	9	7	6.4	8	3	##	Acyltransfer
PF00350	8	7	6	9	11	4	6	8	7	9	5.8	9	2	##	Dynamin_N
PF01636	10	7	10	7	9	7	17	17	4	5	5.0	12	1	##	APH
PF00488	6	6	5	7	6	6	8	6	10	7	5.9	7	4	##	MutS_V
PF02786	6	6	6	6	7	7	6	7	7	9	5.9	8	4	##	CPSase_L_D2
PF00289	6	7	6	6	7	6	6	6	8	7	5.8	7	4	##	CPSase_L_chain
PF08534	7	6	8	6	9	8	6	8	6	8	5.2	8	2	##	Redoxin
PF02854	8	4	6	12	7	5	6	8	6	5	5.2	9	2	##	MIF4G
PF07723	6	8	4	14	4	5	44	9	12	7	3.6	23	0	##	LRR_2
PF05183	12	4	7	7	8	6	6	6	7	8	4.9	11	0	##	RdRP

PF02171	7	7	9	7	7	7	3	4	7	11	4.8	10	0	##	Piwi
PF01070	7	6	6	9	6	7	10	5	9	7	4.7	8	1	##	FMN_dh
PF00689	5	9	7	7	8	4	5	5	4	5	5.0	8	3	##	Cation_ATPaseC
PF00011	6	4	12	4	6	6	5	9	6	6	4.6	11	0	##	HSP20
PF02212	6	6	4	7	9	4	5	6	7	9	4.6	8	1	##	GED
PF04427	5	4	5	5	5	6	5	5	5	5	4.8	5	2	##	Brix
PF00250	5	5	5	9	5	5	5	6	5	5	4.5	8	0	##	Fork_head
PF03061	4	5	5	6	9	2	4	6	4	6	4.6	8	1	##	4HBT
PF00730	5	6	5	6	5	4	6	7	6	5	4.4	6	2	##	HhH-GPD
PF00790	5	5	5	5	5	5	5	5	5	7	4.4	6	2	##	VHS
PF01426	7	6	4	5	5	4	5	5	4	5	4.0	6	1	##	BAH
PF00682	4	3	4	5	5	4	7	4	4	5	4.1	6	3	##	HMGL-like
PF03060	7	5	4	3	5	7	6	5	6	9	3.6	8	1	##	NPD
PF01644	4	5	4	4	4	4	4	5	5	6	4.0	5	2	##	Chitin_synth_1
PF02785	4	4	4	4	5	5	4	5	4	7	3.8	5	2	##	Biotin_carb_C
PF03109	4	4	4	4	4	4	4	6	4	5	3.9	5	3	##	ABC1
PF01417	5	5	5	5	5	5	5	5	4	6	3.6	5	2	##	ENTH
PF00698	3	4	4	12	5	1	8	3	8	7	3.4	10	1	##	Acyl_transf_1
PF01624	4	4	3	5	4	4	5	4	4	4	3.8	4	3	##	MutS_I
PF00092	11	4	4	6	2	7	2	3	4	9	3.3	8	0	##	VWA
PF00254	3	3	3	11	3	3	3	3	3	5	3.7	8	1	##	FKBP_C
PF06470	4	3	3	4	4	4	4	5	3	3	3.8	4	2	##	SMC_hinge
PF08740	4	3	5	11	5	2	4	5	4	4	3.2	6	1	##	BCS1_N
PF01920	5	4	3	4	3	4	4	3	4	4	3.4	4	1	##	Prefoldin_2
PF00652	2	4	2	1	3	0	1	2	0	22	3.4	16	0	##	Ricin_B_lectin
PF00622	4	3	2	3	4	4	4	4	4	7	3.3	4	2	##	SPRY
PF04145	3	4	3	3	4	3	2	3	3	7	3.1	6	1	##	Ctr
PF00615	3	6	3	3	3	3	4	3	4	3	3.1	5	0	##	RGS
PF00403	4	5	4	3	7	4	4	5	4	5	2.6	4	1	##	HMA
PF07249	4	3	6	5	12	1	7	6	6	5	2.2	8	0	##	Ceratoplatanin
PF08033	3	3	3	5	3	3	3	3	3	3	3.0	4	2	##	Sec23_BS
PF01209	5	7	2	2	2	7	4	2	5	3	2.7	6	1	##	Ubie_methyltrn
PF01713	3	2	2	4	3	2	7	3	3	3	2.9	6	1	##	Smr
PF00201	7	4	6	2	7	2	1	19	2	6	2.0	9	0	##	UDPGT
PF08542	3	2	2	3	3	3	3	3	3	4	2.9	3	2	##	Rep_fac_C
PF01975	5	6	5	8	7	3	3	2	4	6	2.1	6	0	##	SurE
PF03876	3	2	3	4	4	3	3	3	3	3	2.7	3	1	##	RNA_pol_Rpb7_N
PF01851	3	3	2	3	3	3	3	3	3	4	2.7	3	2	##	PC_rep

PF02782	3	3	3	3	3	2	3	3	3	4	2.7	3	2	##	FGGY_C
PF01728	3	2	3	5	2	4	7	2	4	3	2.4	6	1	##	FtsJ
PF08325	5	3	3	3	3	3	3	3	3	3	2.4	4	0	##	WLM
PF00174	4	4	3	3	3	4	4	4	6	6	2.0	5	0	##	Oxidored_molyb
PF03914	2	1	3	3	2	3	3	4	2	5	2.4	3	2	##	CBF
PF03226	3	2	3	3	3	3	3	3	3	5	2.2	4	0	##	Yippee
PF08512	3	2	3	2	2	2	2	3	3	4	2.4	3	2	##	Rtt106
PF02777	3	2	3	3	3	4	3	4	2	4	2.2	3	1	##	Sod_Fe_C
PF00474	3	2	2	4	1	3	4	2	6	3	2.2	5	0	##	SSF
PF02386	3	3	2	2	3	2	3	3	6	2	2.1	5	0	##	TrkH
PF04438	5	1	3	4	4	0	2	3	4	3	2.1	3	0	##	zf-HIT
PF03798	2	2	1	2	3	2	2	2	2	4	2.3	3	1	##	LAG1
PF05190	3	3	2	4	3	2	2	3	3	4	2.0	3	1	##	MutS_IV
PF02852	2	2	2	6	2	4	2	2	2	2	2.1	3	2	##	Pyr_redox_dim
PF00641	1	1	3	1	2	1	2	4	13	0	2.0	4	0	##	zf-RanBP
PF00923	2	2	2	2	2	1	2	5	2	2	2.1	4	1	##	Transaldolase
PF08390	2	1	1	2	3	2	2	3	2	4	2.1	3	1	##	TRAM1
PF01507	2	2	2	2	2	5	2	2	2	2	2.0	3	2	##	PAPS_reduct
PF00081	2	4	3	2	2	3	2	3	2	2	1.9	3	0	##	Sod_Fe_N
PF00183	2	3	2	3	2	3	2	2	2	4	1.9	3	0	##	HSP90
PF00445	2	2	2	3	2	2	2	2	2	6	1.9	4	0	##	RibonucleaseT2
PF07651	2	2	2	2	2	2	2	2	1	4	2.0	3	1	##	ANTH
PF05362	2	2	2	2	2	2	2	2	4	2	2.0	3	1	##	Lon_C
PF04053	2	2	2	2	2	2	2	3	2	2	2.0	2	1	##	Coatomer_WDAD
PF00520	2	2	2	2	2	1	2	2	3	5	1.9	4	1	##	Ion_trans
PF01761	3	2	2	3	2	4	2	3	3	5	1.7	4	1	##	DHQ_synthase
PF01521	2	2	2	2	3	1	2	2	2	2	2.0	2	1	##	Fe-S_biosyn
PF08799	2	2	2	2	2	2	2	2	2	3	1.9	2	1	##	PRP4
PF00312	2	2	2	2	2	1	2	2	2	3	1.9	2	1	##	Ribosomal_S15
PF07650	2	1	1	2	2	3	2	2	3	2	1.9	2	1	##	KH_2
PF01846	2	2	2	2	2	2	3	2	2	2	1.9	2	1	##	FF
PF03595	5	3	4	1	4	2	3	3	2	4	1.5	4	0	##	C4dic_mal_tran
PF00849	2	2	1	5	2	2	2	2	2	2	1.8	3	1	##	PseudoU_synth2
PF09378	2	2	2	2	2	2	2	2	2	3	1.8	2	0	##	HAS-barrel
PF01246	2	1	2	2	2	2	2	1	2	3	1.9	2	0	##	Ribosomal_L24e
PF04855	2	2	2	3	2	2	1	2	2	2	1.8	2	1	##	SNF5
PF04825	2	2	2	2	2	1	1	2	2	3	1.8	2	1	##	Rad21_Rec8_N
PF03460	2	7	2	2	2	2	2	2	1	4	1.5	3	0	##	NIR_SIR_ferr

PF03807	3	1	3	2	3	2	3	2	2	4	1.5	3	1	##	F420_oxidored
PF01388	2	1	2	1	1	1	2	1	4	1	1.8	3	1	##	ARID
PF04695	2	2	2	3	2	0	2	2	2	2	1.6	2	1	##	Pex14_N
PF07685	1	2	2	2	2	1	2	4	2	2	1.6	2	0	##	GATase_3
PF04824	2	1	2	2	2	1	1	2	2	3	1.6	2	1	##	Rad21_Rec8
PF01077	2	4	2	2	2	2	2	2	1	1	1.5	3	0	##	NIR_SIR
PF02265	1	2	2	1	2	2	1	2	0	4	1.6	3	0	##	S1-P1_nuclease
PF01137	2	1	2	2	2	1	2	2	4	2	1.5	2	0	##	RTC
PF05189	2	1	2	2	2	1	2	2	3	2	1.5	2	0	##	RTC_insert
PF03070	2	5	1	3	1	1	1	1	2	2	1.4	3	0	##	TENA_THI-4
PF00633	1	1	1	4	2	2	2	0	2	3	1.4	3	0	##	HHH
PF00393	1	2	2	2	1	2	2	2	2	3	1.2	2	1	##	6PGD
PF08354	2	1	1	2	1	2	1	2	2	6	1.2	3	0	##	DUF1729
PF02184	1	2	1	3	1	2	2	1	2	1	1.3	2	1	##	HAT
PF08154	2	1	2	2	2	1	2	3	2	1	1.2	2	0	##	NLE
PF01174	2	2	2	1	2	1	1	4	1	2	1.2	2	0	##	SNO
PF01218	2	2	3	1	3	2	2	1	2	2	1.2	2	0	##	Coprogen_oxids
PF03725	3	1	4	2	2	2	2	3	1	2	1.1	2	0	##	RNase_PH_C
PF03311	2	2	1	1	1	2	1	1	1	3	1.2	2	1	##	Cornichon
PF04992	1	3	1	1	1	1	1	1	1	3	1.1	2	1	##	RNA_pol_Rpb1_6
PF08487	6	1	0	4	0	3	0	1	0	5	0.9	5	0	##	VIT